ELSEVIER

Journal of Organometallic Chemistry 578 (1999) 229–246

Journal of Organometallic Chemistry

Appreciably bent sp carbon chains: synthesis, structure, and protonation of organometallic 1,3,5-triynes and 1,3,5,7-tetraynes of the formula (η^5-C_5Me_5)Re(NO)(PPh_3)((C≡C)$_n$-*p*-C_6H_4Me)

Roman Dembinski [a], Tadeusz Lis [b], Slawomir Szafert [a], Charles L. Mayne [a], Tamás Bartik [a], J.A. Gladysz [a,c,*]

[a] *Department of Chemistry, University of Utah, Salt Lake City, UT 84112, USA*
[b] *Department of Chemistry, University of Wrocław, 14 F. Joliot-Curie, 50-383 Wrocław, Poland*
[c] *Institut für Organische Chemie, Friedrich–Alexander Universität Erlangen–Nürnberg, Henkestrasse 42, 91054 Erlangen, Germany*

Received 25 August 1998

Abstract

The diyne (η^5-C_5Me_5)Re(NO)(PPh_3)(C≡CC≡CSiMe_3) is elaborated to (η^5-C_5Me_5)Re(NO)(PPh_3)(C≡CC≡CC≡CSiR_3) (R = Me, **3a**; Et, **3b**) by sequences involving *n*-$Bu_4N^+F^-$ in aqueous THF to give (η^5-C_5Me_5)Re(NO)(PPh_3)(C≡CC≡CH) (91%), *n*-BuLi/CuI or *t*-BuOCu to give (η^5-C_5Me_5)Re(NO)(PPh_3)(C≡CC≡CCu) (**4**), and coupling with IC≡CSiMe_3 (48%) or BrC≡CSiEt_3 (84–65%). Complex **3b** is similarly converted to (η^5-C_5Me_5)Re(NO)(PPh_3)(C≡CC≡CC≡CH) (88%) and (η^5-C_5Me_5)Re(NO)(PPh_3)(C≡CC≡CC≡CCu) (**6**). Reactions of **4** and **6** with BrC≡C-*p*-C_6H_4Me give the title compounds (η^5-C_5Me_5)Re(NO)(PPh_3)((C≡C)$_n$-*p*-C_6H_4Me) ($n = 3$, **7**; 4, **8**; 77–66%). Optimized one flask conversions of **1a** and **3b** to **7** (81%) and **8** (71%) are described. The crystal structures of **7** (monoclinic, $P2_1/c$, $a/b/c = 17.951(8)/8.377(5)/22.160(9)$ Å, $\beta = 103.63(5)°$, $Z = 4$), and **8** (monoclinic, $P2_1/n$, $a/b/c = 8.426(3)/16.400(6)/25.400(9)$ Å, $\beta = 97.51(3)°$, $Z = 4$) show markedly curved sp carbon chains—much more than hexatriynes or octatetraynes reported to date. The bond angles associated with the Re(C≡C)$_n$C moieties (min/max/avg) are 169.1(10)°/178.8(13)°/174.7° (**7**) and 170.0(9)°/178.8(10)°/175.7° (**8**). Other structural features are normal, and bending is provisionally ascribed to packing forces. Reaction of **7** and HBF_4·OEt_2 gives the cationic vinylidene complex [(η^5-C_5Me_5)Re(NO)(PPh_3)(C=C(H)C≡CC≡C-*p*-C_6H_4Me)]$^+$ BF_4^-, the structure of which is established by extensive NMR analyses.

Keywords: Rhenium; Polyynes; Crystallography; Bent carbon chains

1. Introduction

The previous decade has seen many stunning new breakthroughs in the field of carbon allotropes [1,2]. The importance of this area, as well as specific achievements, were recognized in the 1996 Nobel Prizes in chemistry [2]. One ongoing topic of controversy concerns the polymeric sp carbon allotrope, often termed 'carbyne' [3]. This substance ranks in conceptual importance as a full equal of diamond (sp^3 lattice) and graphite (sp^2 lattice). It should have a linear ground state, but remains difficult to generate, isolate, and characterize. In this context, there has been conjecture that long sp carbon chains might have low energy barriers to bending, and readily convert to various fullerenes [4,5].

We have sought to probe this point with model compounds. In 1997, we surveyed all crystallographically characterized compounds with at least eight consecutive sp hybridized carbons [6]. These included six 1,3,5,7-tetraynes [4b,6,7,8,9,10] and a 1,3,5,7,9-pentayne [11], but no cumulenes. However, none exhibited appre-

* Corresponding author.

0022-328X/99/$ - see front matter © 1999 Elsevier Science S.A. All rights reserved.
PII: S0022-328X(98)01128-0

ciable chain bending. In the meantime, we have continued to structurally characterize all such crystalline compounds synthesized in our laboratory. Many of these serve as intermediates in the preparation of complexes in which sp carbon chains span two transition metals, $[L_nMC_xM'L'_n]$. This separate area of endeavor is currently receiving intense attention in many research groups [12,13].

In this paper, we report the synthesis and crystal structure of the first 1,3,5,7-tetrayne that shows appreciable sp carbon chain bending, as well as a 1,3,5-triyne homolog that is even more deformed. These compounds feature a *p*-C_6H_4Me (*p*-tolyl) group on one terminus, and the chiral rhenium fragment (η^5-C_5Me_5)Re(NO)(PPh_3) (**I**) on the other. The molecular structures and packing motifs are carefully analyzed and compared. The protonation of the triyne ligand is also studied. Attack occurs upon the carbon beta to rhenium to give a cationic vinylidene complex.

2. Results

2.1. Syntheses of polyalkynyl compounds

The 'Cadiot–Chodkiewicz' reaction entails the generation of an alkynyl copper species, followed by coupling with a haloalkyne to give a 1,3-diyne moiety [14]. We have made extensive use of such protocols to extend sp carbon chains in metal co-ordination spheres [6,12b,c]. In connection with several objectives, we sought chains with organorhenium and *p*-tolyl end-groups. Thus, the known bromoalkyne BrC≡C-*p*-C_6H_4Me [15] was prepared in 72% yield by a new route from the corresponding terminal alkyne, NBS, and $AgNO_3$, as described in the experimental section [16]. This compound can be kept for months at −10°C with only slight decomposition.

The required $Re(C{\equiv}C)_nCu$ coupling partners have been described in brief notes or communications [6,12b]. This study was used as an opportunity to fully optimize the synthetic sequence, and provide full details for each step. A key building block, the trimethylsilyl capped butadiynyl complex (η^5-C_5Me_5)Re(NO)-(PPh_3)(C≡CC≡CSiMe_3) (**1a**), was synthesized by deprotonation of a cationic π alkyne complex as described in a full paper [17]. As shown in Scheme 1, **1a** could be converted to the butadiynyl complex (η^5-C_5Me_5)Re(NO)(PPh_3)(C≡CC≡CH) (**2**) in two ways: (1) K_2CO_3 in methanol, a previously reported recipe that requires 8–12 h for completion [18], or (2) *n*-$Bu_4N^+F^-$ (0.2 equivalents; 5% water by weight) in THF, a new protocol that requires only 0.5 h. Workups gave **2** in 91–84% yields.

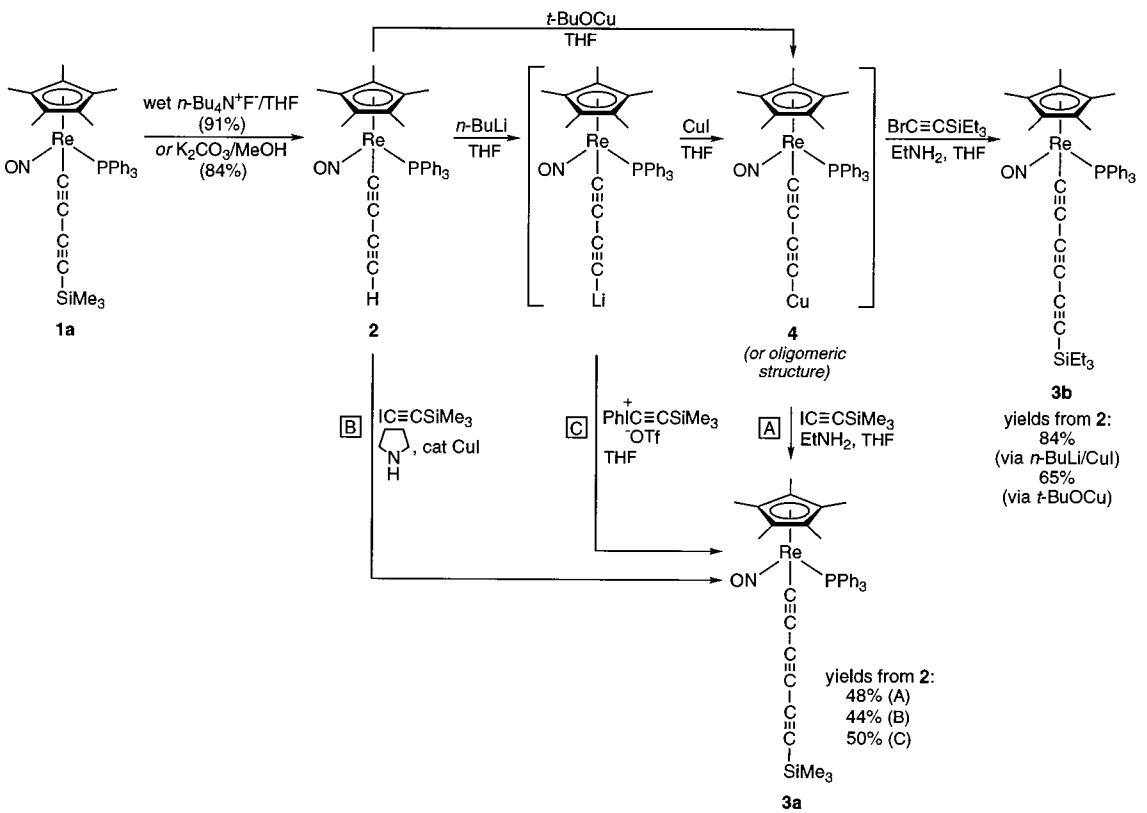

Scheme 1. Syntheses of 1,3,5-hexatriynyl complexes **3a** and **3b**.

The trimethylsilyl capped hexatriynyl complex (η^5-C_5Me_5)Re(NO)(PPh_3)(C≡CC≡CC≡C$SiMe_3$) (**3a**) and triethylsilyl analog (η^5-C_5Me_5)Re(NO)(PPh_3)(C≡CC≡CC≡C$SiEt_3$) (**3b**) were synthesized as summarized in Scheme 1. The former has not been reported earlier. First, **2** was deprotonated with *n*-BuLi (1.05 equivalents, −45°C) in the presence of CuI in THF to generate a species of empirical formula (η^5-C_5Me_5)Re(NO)(PPh_3)(C≡CC≡CCu) (**4**) [6,12b,c,19]. Then an excess of $EtNH_2$ was added (−20°C), followed by the dropwise delivery of IC≡$CSiMe_3$ [20] or BrC≡$CSiEt_3$ [21]. These known haloalkynes were prepared analogously to BrC≡C-*p*-C_6H_4Me. Workups gave **3a** and **3b** in 48 and 84% yields as analytically pure orange and red–brown solids.

Other coupling reactions were explored. Per a recent modification of the Cadiot–Chodkiewicz recipe [22] **2** and IC≡$CSiMe_3$ were reacted in the presence of excess pyrrolidine and a catalytic amount of CuI (Scheme 1, step B). Workup gave **3a** in 44% yield. Alternatively, the iodonium triflate [PhIC≡$CSiMe_3$]$^+$$TfO^-$ was prepared [23] and added to a mixture of **2** and *n*-BuLi (Scheme 1, step C). Alkynyl iodonium salts have previously been utilized in alkyne coupling reactions [24]. Workup gave **3a** in 50% yield. However, **3b** was selected for subsequent preparative studies on the basis of (1) the superior yield, (2) a greater shelf stability, (3) the greater shelf stability of the haloalkyne precursor BrC≡$CSiEt_3$, and (4) the ease of purification. Importantly, the incomplete purification of **3a**,**b** results in workup problems in subsequent steps.

Attention was turned to the title compounds. As shown in Scheme 2, **1a** was again converted to **2** (91–84%) and the copper species **4**, which was treated with BrC≡C-*p*-C_6H_4Me in the presence of excess $EtNH_2$. Workup gave the analytically pure hexatriynyl complex (η^5-C_5Me_5)Re(NO)(PPh_3)(C≡CC≡CC≡C-*p*-C_6H_4Me) (**7**) in 77% yield after crystallization. Analogous reactions were used to convert **3b** to the parent hexatriynyl complex **5** (88–90%) and then the copper species (η^5-C_5Me_5)Re(NO)(PPh_3)(C≡CC≡CC≡CCu) (**6**) [19]. A similar reaction with BrC≡C-*p*-C_6H_4Me gave the 1,3,5,7-octatetraynyl complex (η^5-C_5Me_5)Re(NO)(PPh_3)(C≡CC≡CC≡CC≡C-*p*-C_6H_4Me)(**8**) in 66% yield after workup.

Streamlining of the preceding syntheses was attempted. In an attempt to bypass the use of *n*-BuLi, the copper alkoxide *t*-BuOCu was prepared from *t*-BuOLi and CuCl [25]. Then **1a**, *n*-$Bu_4N^+F^-$ (0.2 equivalents), and *t*-BuOCu (1.5 equivalents) were combined in THF at room temperature. An IR spectrum showed the clean formation of the same alkynyl copper species **4** as generated above. Reaction with BrC≡C-*p*-C_6H_4Me as above gave **7** in 81% yield after workup. This one pot sequence gives a significantly higher overall yield than the two step route (65–70%). A similar series of reactions with **3b** gave **8** in 71% yield. In another variant, **3b**, *n*-$Bu_4N^+F^-$ (0.3 equivalents), *t*-BuOK, and CuI were combined in THF at room temperature. This recipe avoids the prior synthesis of *t*-BuOCu. An IR spectrum showed the formation of the alkynyl copper species **6** [19]. Reaction with BrC≡C-*p*-C_6H_4Me as above gave **8** in 50% yield after workup [26].

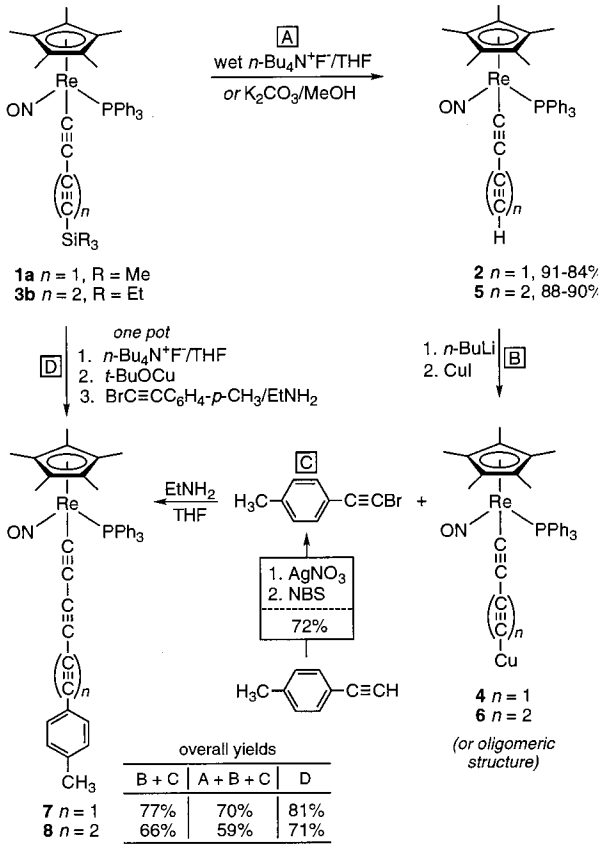

Scheme 2. Syntheses of 1,3,5-hexatriynyl and 1,3,5,7-octatetraynyl complexes **7** and **8**.

The hexatriynyl complexes **3a**,**b**,**5**,**7** and octatetraynyl complex **8** exhibited distinctive spectroscopic properties. IR spectra showed the same number of $\nu_{C\equiv C}$ bands as C≡C linkages (2180–1970 cm^{-1}), and ν_{NO} values close to those of alkynyl complexes of **I** (1659–1650 cm^{-1}). The Re**C**≡**C** ^{13}C-NMR signals appeared at (CD_2Cl_2, ppm) 119.9–112.3 (d, $^2J_{CP}$ 16.4–15.1 Hz) and 112.8–111.2 (s, $^3J_{CP} < 2$ Hz), respectively. The ReC≡C(**C**≡**C**)$_n$C≡CX signals clustered in the range of 61.4–70.0 ppm, a phenomenon analyzed previously [6,12b]. The ReC≡C**C** peaks generally showed phosphorus coupling (d, $^4J_{CP}$ 3.8–2.4 Hz), as observed with lower homologs earlier [17]. The **C**≡**C**Si ^{13}C-NMR signals appeared at 92.7–92.2 and 86.3–83.7 ppm, while the **C**≡**C**-*p*-C_6H_4Me signals were at 78.2–78.0 and 75.5–74.9 ppm. Mass spectra exhibited intense molecular ions. The UV–visible spectra of **7** and **8** are shown

in Fig. 1. As expected, absorptions shift to longer wavelengths and become more intense with increasing chain length. The strongest band of **8** has an exceptionally high molar extinction coefficient, 89 000 $M^{-1}cm^{-1}$. DSC measurements show that **7** and **8** gradually decompose without melting at 181–193°C.

2.2. Crystallography

The crystal structures of **7** and **8** were determined as outlined in Table 1 and described in the experimental section. Refinement afforded the structures in Fig. 2. Selected bond lengths and angles are listed in Table 2, and atomic co-ordinates are given in Table 3. Both sp carbon chains are conspicuously bent. The overlay in Fig. 2 shows that **7** exhibits greater curvature. In order to provide a solid foundation for analysis, the more routine structural features are presented first.

Both **7** and **8** exhibit a formally octahedral rhenium co-ordination geometry, with the cyclopentadienyl ligand occupying three sites. Accordingly, the N–Re–P, P–Re–C41, and N–Re–C41 angles are near 90° (90.2(3)–98.6(5)°). The Re–C41 bond lengths (1.998(12) and 2.016(8) Å) are quite close to that in the 1,3,5,7-tetrayne (η^5-C_5Me_5)Re(NO)(PPh_3)(C≡CC≡CC≡CC≡C$SiMe_3$) (2.037(5) Å), the essentially linear chain of which was analyzed in our earlier study [6]. The C≡C bonds in **8** (1.214(11)–1.242(12) Å) fall into a normal range [27]. However, the ReC≡C linkage in **7** (1.28(2) Å) appears, subject to the larger estimated S.D. value, to be longer. Both complexes give the short ≡C–C≡ sp/sp single bonds (1.33(2)–1.380(11) Å) typical of polyynes, as discussed previously [6]. Key data for **8** and other crystallographically characterized 1,3,5,7-tetraynes are summarized in Table 4.

The four sp C–C–C bond angles in **7** range from 171.6(12)° to 178.8(13)°, with an average of 174.2°. The Re–C≡C linkage is especially bent (169.1(10)°). However, the C≡C–tolyl linkage at the opposite terminus is nearly linear (177.1(12)°). The average of all six angles is 174.7°. As summarized in Table 4, the Re–C≡C, CCC, and C≡C–tolyl angles in **8** average 175.7°. This is significantly lower than the corresponding averages in other structurally characterized tetraynes. The Re**C**≡**C**–**C** linkage shows the greatest bending (170.0(9)°, vs. 171.6(12)° in **7**). Another way to analyze curvature is to compare the actual distance between the endgroups with the sum of the bond lengths connecting them. The **Re**(C≡C)$_3$**C** termini in **7** are separated by 9.69(2) Å, and the intervening bond lengths total 9.87 Å. The corresponding values for **8** are 12.22(1) and 12.42 Å. Also,

Table 1
Summary of crystallographic data for **7** and **8**[a]

	7	**8**
Molecular formula	$C_{41}H_{37}NOPRe$	$C_{43}H_{37}NOPRe$
Molecular weight	776.89	800.91
Crystal system	Monoclinic	Monoclinic
Space group	$P2_1/c$	$P2_1/n$
Temperature of collection (K)	120(1)	120(1)
Cell dimensions (120(1) K)		
a (Å)	17.951(8)	8.426(3)
b (Å)	8.377(5)	16.400(6)
c (Å)	22.160(9)	25.400(9)
β (°)	103.63(5)	97.51(3)
V (Å^3)	3239(3)	3480(3)
Z	4	4
D_{calc} (g cm^{-3}) (120(1) K)	1.593(1)	1.529(1)
Crystal dimensions (mm)	0.2 × 0.2 × 0.04	0.26 × 0.16 × 0.07
Reflections measured	5115	5674
Range/indices (h, k, l)	−22, 21; 0, 10; 0, 27	−10, 10; 0, 20; 0, 31
θ limit (°)	2.33–26.06	2.04–26.05
Total no. of unique data	4976	5582
No. of observed data, $I>2\sigma(I)$	2563	3274
Abs. Coefficient (mm^{-1})	3.84	3.57
Min. transmission (%)	0.494	0.534
Max. transmission (%)	0.858	0.763
No. of variables	396	424
Goodness of fit (all, observed)	1.004, 1.195	1.007, 1.167
R_{int}	0.0633	0.0230
$R = \Sigma\|\|F_o\|-\|F_c\|\|/\Sigma\|F_o\|$ (all, observed)	0.1444, 0.0385	0.1051, 0.0314
$wR_2 = (\Sigma[w(F_o^2-F_c^2)^2]/\Sigma w[F_o^4]^{1/2}$ (all, observed)	0.1037, 0.0852	0.0866, 0.0747
Δ/σ (max)	0.001	−0.001
$\Delta\rho$ (max) (e Å^{-3})	2.21 (ca. 0.86 Å from Re)	1.13 (ca. 1.42 Å from Re)

[a] Data common to both structures: diffractometer, KUMA KM4; radiation λ, Mo–K_α (0.71073 Å); data collection method, $\omega-2\theta$; no. of reflections between std, 100.

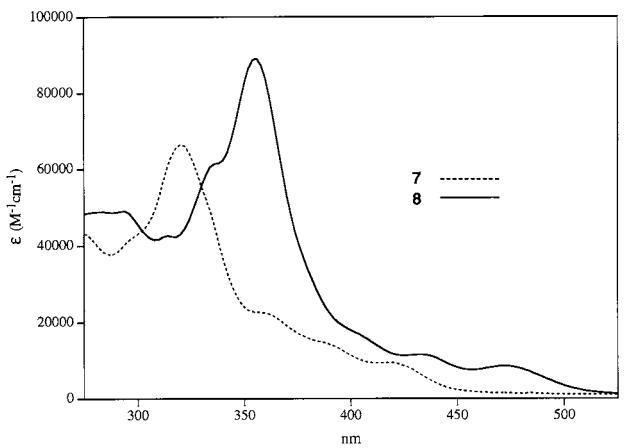

Fig. 1. UV–visible spectra of **7** and **8** (CH_2Cl_2, ambient temperature).

the actual and 'calculated' C≡CC≡CC≡CC≡C distances in **8** can be compared with those in other 1,3,5,7-tetraynes. As summarized in Table 4, **8** exhibits the largest difference to date (8.89(2) vs. 8.97 Å).

The curvature in **7** and **8** was next analyzed by taking vectors between the Re(C≡C)$_n$C termini, and computing angles with vectors defined by the termini and every atom in the chain. Results are summarized in Fig. 3. Atoms are bent as much as 17° out of the direct line connecting the endgroups. The sense of the curvature continues through the *p*-tolyl groups, one measure of which are the angles defined by the two substituted carbons and the methyl groups (∠C51–C54–C57: 177.3°, 177.8°). We were also curious about how the C41–Re–C51 angles would change when C41 was moved to an idealized octahedral position with respect

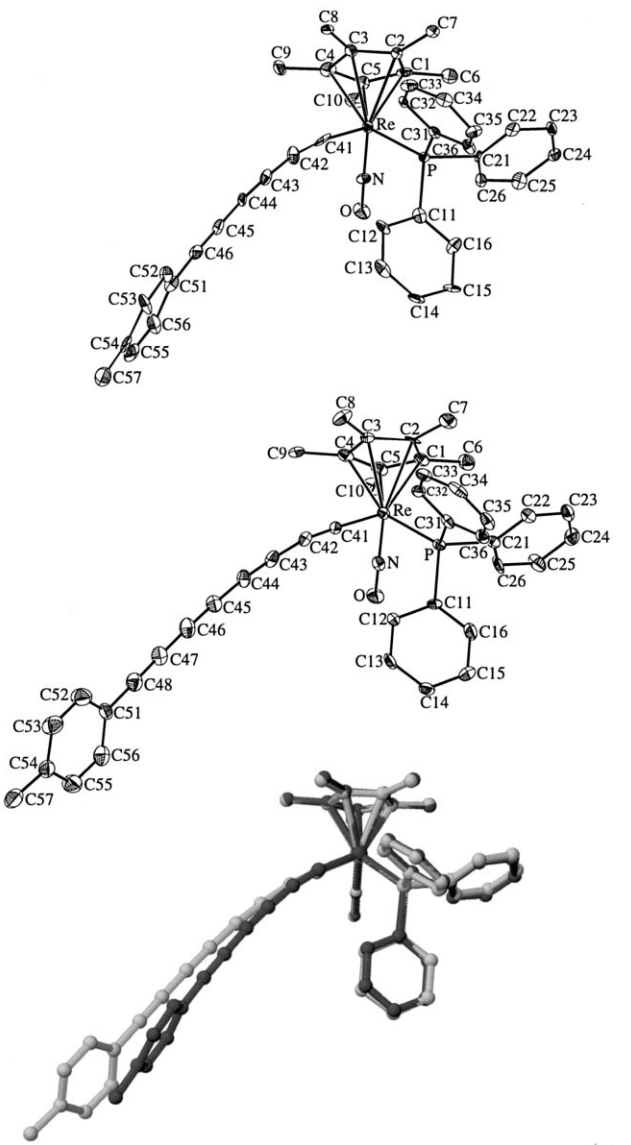

Fig. 2. Structures of **7** (top), **8** (middle), and a superposition (bottom).

Table 2
Selected bond lengths and angles in **7** and **8**

	7	**8**
Bond lengths (Å)		
Re–P	2.366(3)	2.380(2)
Re–N	1.799(10)	1.761(6)
N–O	1.163(11)	1.204(8)
Re–C41	1.998(12)	2.016(8)
Re–C1	2.333(12)	2.309(8)
Re–C2	2.375(11)	2.380(6)
Re–C3	2.357(11)	2.349(7)
Re–C4	2.278(11)	2.263(7)
Re–C5	2.248(10)	2.243(8)
P–C11	1.831(12)	1.842(7)
P–C21	1.848(10)	1.831(8)
P–C31	1.826(11)	1.838(8)
C41–C42	1.28(2)	1.214(11)
C42–C43	1.35(2)	1.380(11)
C43–C44	1.23(2)	1.233(11)
C44–C45	1.33(2)	1.338(11)
C45–C46	1.22(2)	1.242(12)
C46–C51	1.46(2)	–
C46–C47	–	1.337(12)
C47–C48	–	1.223(11)
C48–C51	–	1.439(12)
C51–C52	1.40(2)	1.360(13)
C51–C56	1.39(2)	1.389(11)
C52–C53	1.36(2)	1.383(13)
C53–C54	1.39(2)	1.376(13)
C54–C55	1.35(2)	1.396(13)
C54–C57	1.53(2)	1.514(12)
C55–C56	1.40(2)	1.388(12)
Bond angles (°)		
N–Re–P	91.1(3)	91.4(2)
P–Re–C41	90.2(3)	92.0(2)
N–Re–C41	98.6(5)	95.5(3)
Re–N–O	175.9(9)	175.5(6)
C1–Re–C41	146.5(4)	147.9(3)
C2–Re–C41	114.8(4)	115.7(3)
C3–Re–C41	87.9(4)	88.5(3)
C4–Re–C41	93.6(4)	93.5(3)
C5–Re–C41	129.5(4)	128.1(3)
Re–C41–C42	169.1(10)	174.5(7)
C41–C42–C43	171.6(12)	170.0(9)
C42–C43–C44	176.7(12)	176.9(9)
C43–C44–C45	174.7(11)	173.6(10)
C44–C45–C46	178.8(13)	178.1(10)
C45–C46–C51	177.1(12)	–
C45–C46–C47	–	177.6(10)
C46–C47–C48	–	178.8(10)
C47–C48–C51	–	175.8(10)
C46–C51–C52	119.2(12)	–
C46–C51–C56	122.0(11)	–
C48–C51–C52	–	122.3(8)
C48–C51–C56	–	119.1(9)
C51–C52–C53	120.1(12)	121.6(9)
C51–C56–C55	118.3(12)	119.6(9)
C52–C51–C56	118.7(11)	118.6(8)
C52–C53–C54	122.5(11)	121.6(10)
C53–C54–C55	116.2(11)	116.5(9)
C53–C54–C57	120.3(13)	119.9(9)
C54–C55–C56	124.1(14)	122.1(9)
C55–C54–C57	123.4(14)	123.6(9)
C11–P–C21	103.3(5)	103.0(3)
C11–P–C31	96.5(5)	98.7(3)
C21–P–C31	105.8(5)	105.6(3)

to the N–Re–P plane. We had expected that values would increase, analogous to taking a bent metal saw and releasing one end to re-establish the planar equilibrium state. To our surprise, the angles decreased from 17.7(3) and 17.08(21)° to 11.10 and 11.28°.

Although we were not optimistic that a simple 'one parameter' explanation for chain curvature could be identified, various possibilities were probed. For example, the resonance relationship **II**↔**III** in Scheme 3 was considered. Zwitterionic vinylidene resonance contributors such as **III** have often been invoked to account for the pronounced nucleophilicity of the beta carbon of many neutral alkynyl complexes [28]. In extreme cases, bending might occur as in **IV**. The structures of vinyli-

Table 3
Atomic coordinates and equivalent isotropic thermal parameters of located atoms in **7** and **8**

	7				**8**			
	x	*y*	*z*	U_{eq}	*y*	*z*	U_{eq}	
Re	0.61843(3)	0.66994(7)	0.62635(2)	0.01456(12)	0.73341(3)	0.52137(2)	0.619208(11)	0.01737(8)
P	0.72854(13)	0.6625(4)	0.70960(10)	0.0138(5)	0.7878(2)	0.56088(12)	0.70994(8)	0.0183(4)
N	0.5798(5)	0.4960(12)	0.6557(4)	0.018(2)	0.5695(7)	0.4616(4)	0.6324(2)	0.021(2)
O	0.5513(5)	0.3893(10)	0.6751(4)	0.031(2)	0.4613(6)	0.4165(4)	0.6392(2)	0.0346(15)
C1	0.5547(7)	0.9009(15)	0.6450(5)	0.023(3)	0.9520(9)	0.4422(6)	0.6067(3)	0.023(2)
C2	0.6152(7)	0.9527(13)	0.6187(5)	0.015(3)[a]	1.0064(7)	0.5266(6)	0.6045(3)	0.022(2)
C3	0.6044(6)	0.8904(14)	0.5585(5)	0.021(3)	0.9146(8)	0.5651(5)	0.5622(3)	0.021(2)
C4	0.5360(6)	0.7921(14)	0.5456(5)	0.026(3)	0.8001(8)	0.5062(5)	0.5363(3)	0.024(2)
C5	0.5065(6)	0.8026(14)	0.6011(4)	0.021(2)[a]	0.8246(9)	0.4308(5)	0.5642(3)	0.027(2)
C6	0.5416(7)	0.9583(15)	0.7062(5)	0.028(3)	1.0351(9)	0.3755(5)	0.6418(3)	0.031(2)
C7	0.6741(6)	1.0804(14)	0.6472(5)	0.023(3)	1.1504(9)	0.5612(6)	0.6385(3)	0.033(2)
C8	0.6495(6)	0.9236(13)	0.5115(5)	0.021(3)	0.9318(11)	0.6506(6)	0.5420(3)	0.037(2)
C9	0.4998(7)	0.7216(14)	0.4846(5)	0.026(3)	0.6973(8)	0.5240(6)	0.4845(3)	0.032(2)
C10	0.4313(6)	0.7311(15)	0.6081(6)	0.032(3)	0.7432(10)	0.3511(5)	0.5503(4)	0.035(2)
C11	0.7727(6)	0.4701(14)	0.7362(5)	0.020(3)	0.6173(8)	0.5767(5)	0.7474(3)	0.019(2)
C12	0.7995(6)	0.3782(13)	0.6942(6)	0.022(3)	0.4894(8)	0.6244(5)	0.7239(3)	0.023(2)
C13	0.8453(6)	0.2460(15)	0.7154(6)	0.028(3)	0.3730(9)	0.6503(5)	0.7536(3)	0.027(2)
C14	0.8615(6)	0.2034(13)	0.7761(5)	0.025(3)	0.3788(9)	0.6275(5)	0.8063(3)	0.026(2)
C15	0.8334(6)	0.2897(12)	0.8183(6)	0.023(3)	0.5036(10)	0.5783(6)	0.8288(3)	0.037(2)
C16	0.7890(7)	0.4275(16)	0.7980(5)	0.026(3)	0.6202(9)	0.5526(5)	0.7990(3)	0.032(2)
C21	0.7065(6)	0.7476(13)	0.7804(4)	0.010(2)	0.9046(7)	0.4818(5)	0.7484(2)	0.0181(14)
C22	0.7371(6)	0.8878(14)	0.8060(5)	0.020(3)	1.0607(8)	0.4915(5)	0.7718(3)	0.022(2)
C23	0.7127(7)	0.9505(15)	0.8573(5)	0.025(3)	1.1454(9)	0.4278(5)	0.7972(3)	0.028(2)
C24	0.6603(6)	0.8681(13)	0.8814(5)	0.022(3)	1.0715(10)	0.3522(6)	0.7997(3)	0.033(2)
C25	0.6293(6)	0.7296(15)	0.8544(5)	0.026(3)	0.9152(10)	0.3405(6)	0.7764(4)	0.036(2)
C26	0.6511(5)	0.6738(18)	0.8029(4)	0.018(2)	0.8342(9)	0.4060(5)	0.7508(3)	0.031(2)
C31	0.8162(6)	0.7614(13)	0.7013(5)	0.016(2)	0.8949(8)	0.6569(4)	0.7268(3)	0.020(2)
C32	0.8801(6)	0.7698(13)	0.7497(5)	0.021(3)	0.9407(9)	0.6792(5)	0.7798(3)	0.023(2)
C33	0.9491(6)	0.8275(18)	0.7413(5)	0.025(2)	1.0118(9)	0.7532(5)	0.7926(3)	0.028(2)
C34	0.9525(6)	0.8859(13)	0.6836(5)	0.023(3)	1.0418(9)	0.8053(5)	0.7526(4)	0.030(2)
C35	0.8906(6)	0.8756(13)	0.6342(5)	0.026(3)	0.9981(8)	0.7849(5)	0.7007(3)	0.028(2)
C36	0.8218(5)	0.8123(15)	0.6420(4)	0.014(2)	0.9228(8)	0.7111(5)	0.6878(3)	0.022(2)
C41	0.6763(6)	0.5608(15)	0.5714(5)	0.023(3)	0.6046(8)	0.6232(5)	0.6003(3)	0.021(2)
C42	0.7092(6)	0.4669(15)	0.5405(5)	0.025(3)	0.5159(9)	0.6803(5)	0.5877(3)	0.026(2)
C43	0.7473(6)	0.3554(15)	0.5158(4)	0.020(3)	0.3964(10)	0.7380(5)	0.5782(3)	0.028(2)
C44	0.7825(7)	0.2489(14)	0.4958(5)	0.020(3)	0.2875(10)	0.7888(5)	0.5721(3)	0.028(2)
C45	0.8197(6)	0.1257(14)	0.4787(5)	0.022(3)	0.1591(10)	0.8375(5)	0.5676(3)	0.031(2)
C46	0.8525(7)	0.0114(15)	0.4632(5)	0.023(3)	0.0400(10)	0.8826(5)	0.5651(3)	0.035(2)
C47	–	–	–	–	–0.0909(10)	0.9290(5)	0.5638(3)	0.033(2)
C48	–	–	–	–	–0.2118(10)	0.9704(6)	0.5632(3)	0.035(2)
C51	0.8942(7)	–0.1256(15)	0.4476(5)	0.028(3)	–0.3467(8)	1.0240(6)	0.5638(3)	0.030(2)
C52	0.9630(7)	–0.1009(15)	0.4298(5)	0.024(3)	–0.3455(12)	1.1025(7)	0.5465(4)	0.050(3)
C53	1.0044(7)	–0.2278(15)	0.4176(6)	0.031(3)	–0.4785(12)	1.1522(6)	0.5456(4)	0.046(3)
C54	0.9791(7)	–0.3846(16)	0.4187(5)	0.030(3)	–0.6194(11)	1.1241(6)	0.5607(3)	0.036(2)
C55	0.9129(8)	–0.4056(18)	0.4363(5)	0.040(4)	–0.6193(12)	1.0438(6)	0.5790(4)	0.046(3)
C56	0.8685(8)	–0.2808(16)	0.4510(6)	0.036(4)	–0.4855(10)	0.9939(6)	0.5808(3)	0.040(2)
C57	1.0285(9)	–0.5225(18)	0.4054(6)	0.049(4)	–0.7636(12)	1.1798(7)	0.5574(4)	0.049(3)

[a] Refinement as U_{iso}.

Table 4
Summary of bond lengths (Å) and bond angles (°) for crystallographically characterized 1,3,5,7-tetraynes XC≡CC≡CC≡CC≡CX′[a]

X/X′	Ph/Ph[b]	Ph/C≡CPh[c]	*t*-Bu/*t*-Bu	Me_3Si/Me_3Si	Cycbu/Cycbu[d]	Re[e]/$SiMe_3$	Fc/Fc[f]	Re[e]/ *p*-tolyl (**8**)
Bond lengths (Å)								
C1–C2	1.19	1.192	1.217(9)	1.20(1)	1.19(2)	1.208(9)	1.19(1)	1.214(11)
C2–C3	1.36	1.369	1.377(9)	1.39(1)	1.38(3)	1.35(1)	1.38(1)	1.380(11)
C3–C4	1.22	1.206	1.172(8)	1.20(1)	1.18(2)	1.21(1)	1.188(9)	1.233(11)
C4–C5	1.32	1.368	1.351(9)	1.33(1)	1.38(4)	1.36(1)	1.37(1)	1.338(11)
C5–C6	1.22	1.208	1.218(9)	1.20(1)	1.18(2)	1.194(9)	1.188(9)	1.242(12)
C6–C7	1.36	1.368	1.36(1)	1.378(9)	1.38(3)	1.37(1)	1.38(1)	1.337(12)
C7–C8	1.19	1.206	1.202(8)	1.209(9)	1.19(2)	1.20(1)	1.19(1)	1.223(11)
C1–C8 distance sum	–	8.915	8.87	8.88	8.86	8.872(9)	8.88	8.89(2)
C1–C8 bond lengths	8.86	8.917	8.90	8.91	8.88	8.89	8.88	8.97
Bond angles[b] (°)								
X–C1–C2	–	178.08(6)	178.8(6)	178.1(6)	176(2)	176.4(6)	179.5(5)	174.5(7)
C1–C2–C3	–	178.49	177.6(6)	177.7(8)	177(3)	177.4(8)	177.9(6)	170.0(9)
C2–C3–C4	–	178.30	178.5(5)	177.4(7)	179(3)	178.2(8)	179.6(6)	176.9(9)
C3–C4–C5	–	178.67	177.4(6)	177.8(8)	174(3)	176.4(8)	179.6(6)	173.6(10)
C4–C5–C6	–	178.52	176.7(6)	176.9(8)	174(3)	178.9(8)	179.6(6)	178.1(10)
C5–C6–C7	–	178.52	178.9(6)	178.4(7)	179(3)	175.9(8)	179.6(6)	177.6(10)
C6–C7–C8	–	178.67	176.1(6)	178.6(7)	177(3)	179(1)	177.9(6)	178.8(10)
C7–C8–X′	–	178.30	179.4(6)	177.2(6)	176(2)	178.0(9)	179.5(5)	175.8(10)
Average angle	–	178.4	177.9	177.8	176.7	177.5	179.2	175.7
Reference	[7]	[11]	[4b]	[8]	[9]	[6]	[10]	This work

[a] All estimated S.D. values are as reported in the citation provided, or rounded downward by one significant digit.
[b] No bond angles or atomic co-ordinates were reported for X/X′ = Ph/Ph.
[c] Additional data for diphenyl 1,3,5,7,9-pentayne: C8–C9 1.369 Å; C9–C10 1.192 Å; ∠C8–C9–C10 178.49°; ∠C9–C10–Ph 178.08(6)°.
[d] Cycbu = (η^5-C_5H_5)Co(η^4-C(SiMe$_3$)=C(SiMe$_3$)–C(SiMe$_3$)=C–).
[e] Re = (η^5-C_5Me_5)Re(NO)(PPh_3).
[f] Fc = ferrocene.

dene complexes of **I** or cyclopentadienyl homologs have been extensively studied [29–32]. As would be expected from the rhenium fragment HOMO (Scheme 3) and frontier orbital considerations, they exhibit Re=C=C conformations very close to that of the idealized structure **V**. Thus, one question is whether the chains in **7** or **8** curve in the direction of the Re=C=**C** substituents in **V**.

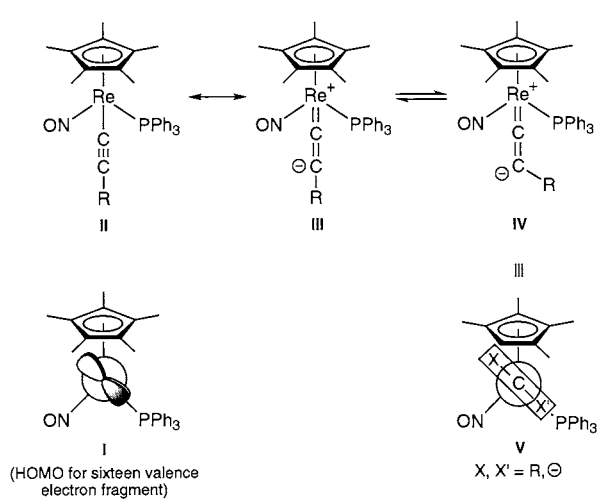

Scheme 3. Possible resonance issues in chain bending.

Fig. 4 shows the corresponding Newman-type projections down the C42–Re vectors of **7** and **8**. The P–Re–C42–C43 torsion-type angles in **V** are 0 and 180°. The corresponding angles in **7** and **8** are

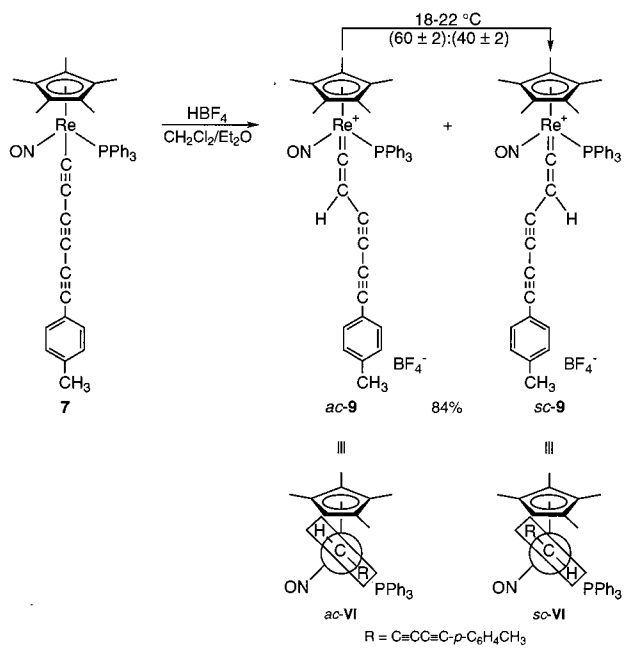

Scheme 4. Protonation of **7**.

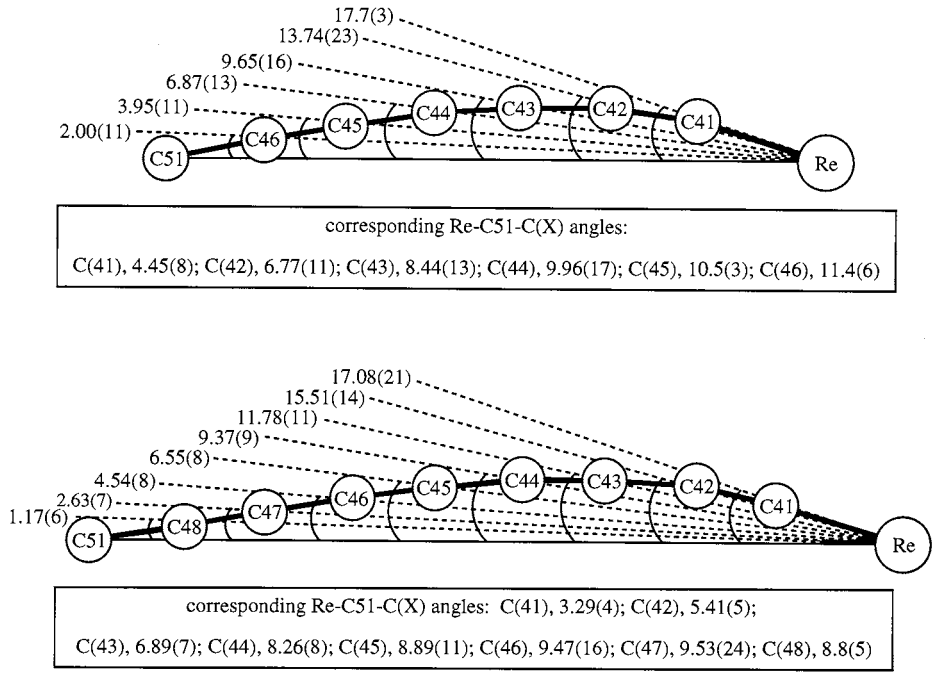

Fig. 3. Angles (°) defined by the Re–C51 vectors and sp carbon atoms in **7** (top) and **8** (bottom).

roughly orthogonal (62.4–83.8°). Hence, the curvature does not have a stereoelectronic origin. We next carefully studied the crystal packing, and among the many views examined found those in Figs. 5 and 6 instructive. These show infinite stacks, with the tolyl rings in approximate edge-on orientations. The sp carbon chains curve *away* from the phenyl rings of a stack of PPh_3 ligands, and *towards* a complementary stack of sp carbon chains. The tolyl endgroups of the two stacks are in close proximity, and define approximately parallel planes separated by 3.0–3.5 Å. However, the tolyl groups lie nearer to the terminal C≡C linkage of the complementary chain. From these data, we suggest that crystal packing forces provide the dominant basis for chain curvature.

2.3. Protonation of 7

The preceding analysis suggests that the chain curvature evident in Figs. 2–6 may not exist in solution. Nonetheless, we were curious about possible reactivity correlations. As noted above, electrophiles attack alkynyl complexes of **I** at the beta carbon to give cationic vinylidene complexes [29,32] With longer polyalkynyl chains as in **7** and **8**, would attack involve a carbon remote from the bulky rhenium center, or the potentially distorted region nearer to rhenium? We were unable to develop any clean reactions with alkylating agents, for which there would be a high probability of kinetic control. Hence, we turned to protonating agents, for which the possibility of rapid and reversible addition would be greater.

As shown in Scheme 4, the hexatriyne **7** and an equimolar amount of $HBF_4{\cdot}OEt_2$ were combined in CD_2Cl_2 in an NMR tube at −80°C. Both ^{1}H- and ^{31}P-NMR spectra showed the formation of two species with closely corresponding chemical shifts in a (87 ± 2):(13 ± 2) ratio (−80°C, major/minor: ^{1}H (δ) 5.92/5.98 =C=CH, 2.30/2.33 $C_6H_4\underline{\mathbf{Me}}$, 1.87/1.90 C_5Me_5; ^{31}P (ppm) 25.2/25.5). The δ 5.92/5.98 ^{1}H signals were close to those of vinylidene and isomeric methylvinylidene complexes of **I** prepared earlier (Re=C=CHH′, δ 5.28, 4.95, $CDCl_3$; Re=C=C(**H**)CH_3, δ 5.91/5.61 *ac*/*sc*, CD_2Cl_2; these data at ambient probe temperature) [31,32]. When samples were warmed to room temperature, equilibration to (60 ± 2):(40 ± 2) mixtures of isomers occurred. This ratio remained unchanged after two days, or when samples were recooled to −80°C. The fact that the kinetic ratio differs from thermodynamic ratio suggests that the protonation is under kinetic control.

Workup of a preparative reaction gave a yellow powder that was provisionally assigned as a mixture of Re=C=C geometric isomers of the vinylidene complex $[(\eta^5\text{-}C_5Me_5)Re(NO)(PPh_3)(C{=}C(H)C{\equiv}CC{\equiv}C\text{-}p\text{-}C_6H_4\text{-}Me)]^+BF_4^-$ (**9**, 84%). Complex **9** was characterized by IR and ^{1}H-, ^{13}C-, and ^{31}P-NMR spectroscopy, all of which supported the proposed formulation. For example, the Re=C=CH ^{1}H-NMR signals showed phosphorus couplings similar to those of other vinylidene complexes of **I** (CD_2Cl_2, major/minor: δ 5.88/5.73, d,

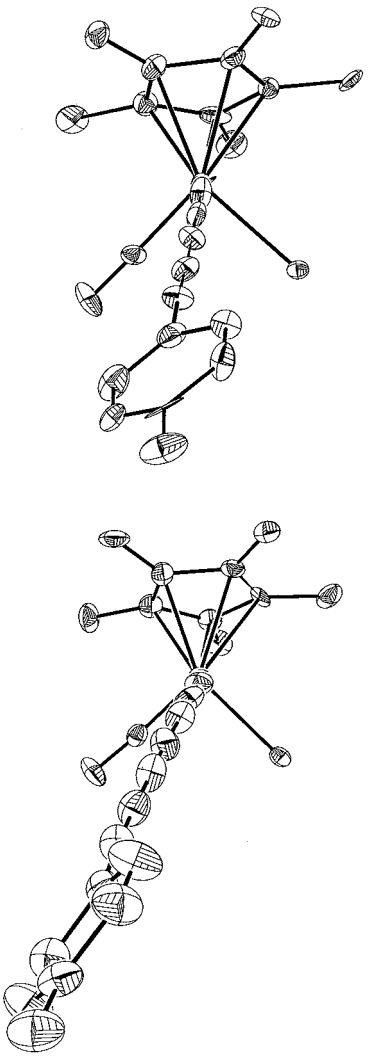

Fig. 4. Newman-type projections down the C42–Re linkages in **7** (top) and **8** (bottom) with PPh_3 phenyl rings omitted.

$^4J_{HP}$ 2.39/2.04 Hz) [31,32]. The ^{13}C-NMR spectrum showed diagnostic Re=**C**=**C** signals (342.7/341.1, d, $^2J_{CP}$ 10.4/10.8 Hz; 112.2/112.8, d, $^3J_{CP}$ 4.0/3.8 Hz), and four peaks that were assigned to the C≡CC≡C linkage (87.0/87.2 s, 86.9/86.3 s, 73.2/73.2 s, 64.8/65.4 s).

The major and minor isomers were tentatively assigned the *ac* and *sc* geometries shown in Scheme 4. This was based upon the relative chemical shifts of the Re=C=CH ^{1}H-NMR signals *at room temperature* [33]. This correlation has been confirmed by crystallographic and by isotope labeling studies, and is derived from the shielding effect of a PPh_3 phenyl ring unique to the *sc* isomer [29,31]. The attack of electrophiles upon the beta carbon of chiral rhenium alkynyl complexes is commonly highly stereoselective [29,32]. As analyzed earlier, the initial formation of an *ac* isomer entails protonation from a direction opposite to the bulky PPh_3 ligand. This provides another argument that the chain proton in **9** is not at a more remote location, as lower stereoselectivity would have been expected. In the cyclopentadienyl series, the thermodynamic isomer is opposite from the kinetic isomer. However, in the pentamethylcyclopentadienyl series, the substituent positions appear to be comparably congested. Accordingly, the methylvinylidene complex of **I** gives a (57 ± 2):(43 ± 2) equilibrium mixture of *ac*/*sc* isomers [31].

We sought to confirm the structure of **9** crystallographically. The corresponding PF_6^- and SbF_6^- salts were generated by the reaction of **7** and $HBF_4{\cdot}OEt_2$ in the presence of the excesses of $NH_4^+PF_6^-$ and $Na^+SbF_6^-$. However, numerous efforts to obtain single crystals were unsuccessful. Such difficulties are not unusual with mixtures of geometric isomers. Hence, we attempted to establish the position of the chain proton by 2D NMR methods, under conditions described in Section 4.

As shown in Fig. 7 (top), a ^{1}H-^{13}C-HMQC experiment [34] correlated the δ 5.88 and 5.73 ^{1}H signals (d, *ac*/*sc*) to the 112.2 and 112.8 ppm ^{13}C signals (the ^{1}H signals in the 1D spectrum fall in the midpoint of the ^{13}C-coupled cross peaks). As noted above, the latter can confidently be assigned to the Re=C=**C** carbons based upon chemical shift and J_{CP} values. This experiment confirms that the carbon and hydrogen atoms responsible for these signals are directly bound. Supporting HMBC experiments [34] were also conducted. The middle spectrum in Fig. 7 shows that the δ 5.88 ^{1}H-NMR signal and 342.7 ppm Re=C signal belong to the same isomer, and that the δ 5.73 ^{1}H-NMR signal and 341.1 ppm Re=C signal belong to the same isomer. This confirms what is otherwise available from the modestly biased integral ratios. The bottom spectrum in Fig. 7 provides the same correlation between the ^{1}H signals and the Re=C=C(H)**C**≡**CC**≡**C** carbons.

Finally, in a particularly demanding experiment, a 2D ^{13}C-INADEQUATE spectrum [35] was acquired over the course of 5 days at -90°C. This technique provides both carbon connectivity and $^1J_{^{13}C^{13}C}$ values. Data are summarized graphically in Chart 1, and show that the =C(H) carbons are connected to four carbon chains that terminate with a *p*-C_6H_4Me moiety. This unequivocally eliminates the possibility of $^+$Re=C=C=C=C(H)C≡C or $^+$Re=C=C=C=C=C=C(H) systems. The $^1J_{^{13}C^{13}C}$ values within the sp hybridized C≡C–C≡C segment are comparable to those of butadiyne (199–205 and 161 vs. 190–194 and 153–155 Hz) [36]. The values for the sp/sp^2 linkages are, as expected, smaller (92–99 Hz).

Summary of 2D ^{13}C INADEQUATE data for **9** (CD_2Cl_2, -90 °C)

Re=C=C(H)—C≡C—C≡C—C_6H_4-*p*-Me

major isomer, *ac*							
chemical shift:	112.00	64.61	85.44	72.43	85.61	117.29	ppm
($^1J_{^{13}C^{13}C}$)		(99.27)	(204.59)	(161.47)	(198.52)	(92.14)	(Hz)
minor isomer, *sc*							
chemical shift:	112.70	65.09	84.89	72.56	85.83	117.29	ppm
($^1J_{^{13}C^{13}C}$)		(97.43)	(203.96)	(160.92)	(201.66)	(92.17)	(Hz)

Chart 1.

3. Discussion

Scheme 2 summarizes highly optimized routes to the title 1,3,5-hexatriynyl and 1,3,5,7-octatetraynyl complexes in which a variant of the Cadiot–Chodkiewicz reaction plays a pivotal role. In very recent work, Bruce has prepared a tungsten 1,3-butadiynyl complex with a *p*-tolyl endgroup [13c]. He started with the corresponding 1,3-butadiynyl complex and employed Sonogashira conditions—*p*-iodotoluene, an amine, and a mixed Cu(I)/Pd(0) catalyst. Other iodoarenes as well as molybdenum precursors also worked well. We anticipate that similar reactions would be successful with our rhenium complexes. However, couplings in which both partners have alkynyl segments constitute more convergent approaches to sp carbon chain extension.

The supporting studies in Scheme 1 also illustrate several important points. Three different coupling reactions (A–C) were evaluated as routes to the trimethylsilyl capped 1,3,5-triene **3a**. Although yields were similar, the Cadiot–Chodkiewicz variant involving a preformed copper alkynyl complex (A) proved superior. However, in our experience it is difficult to predict in advance the best recipe for sp/sp carbon–carbon bond forming reactions, and it is always best to assay several conditions. This is particularly true for oxidative self-couplings of terminal alkynes. The discovery that *t*-BuOCu is sufficiently basic to deprotonate **2** to **4** simplifies the overall procedure. This reagent similarly reacts with the ethynyl complex (η^5-C_5Me_5)Re(NO)-

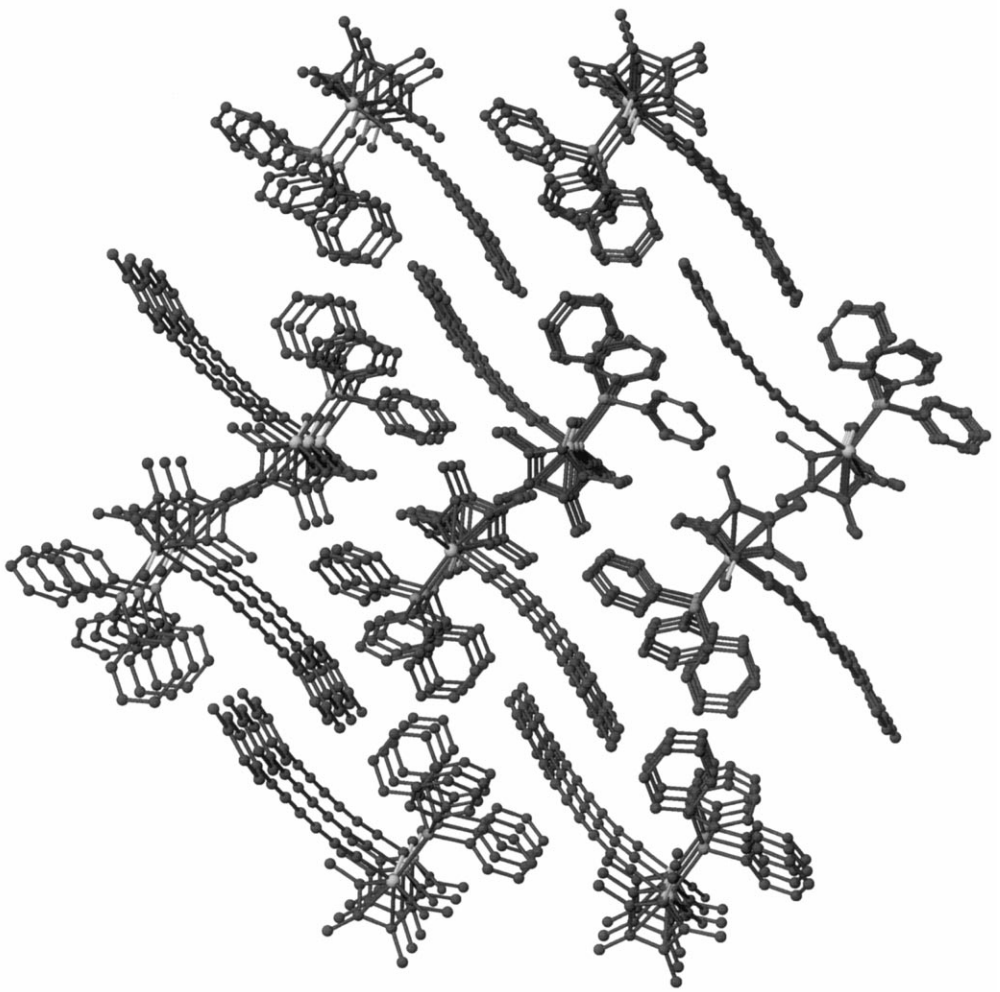

Fig. 5. Representative packing diagram for crystalline **7**.

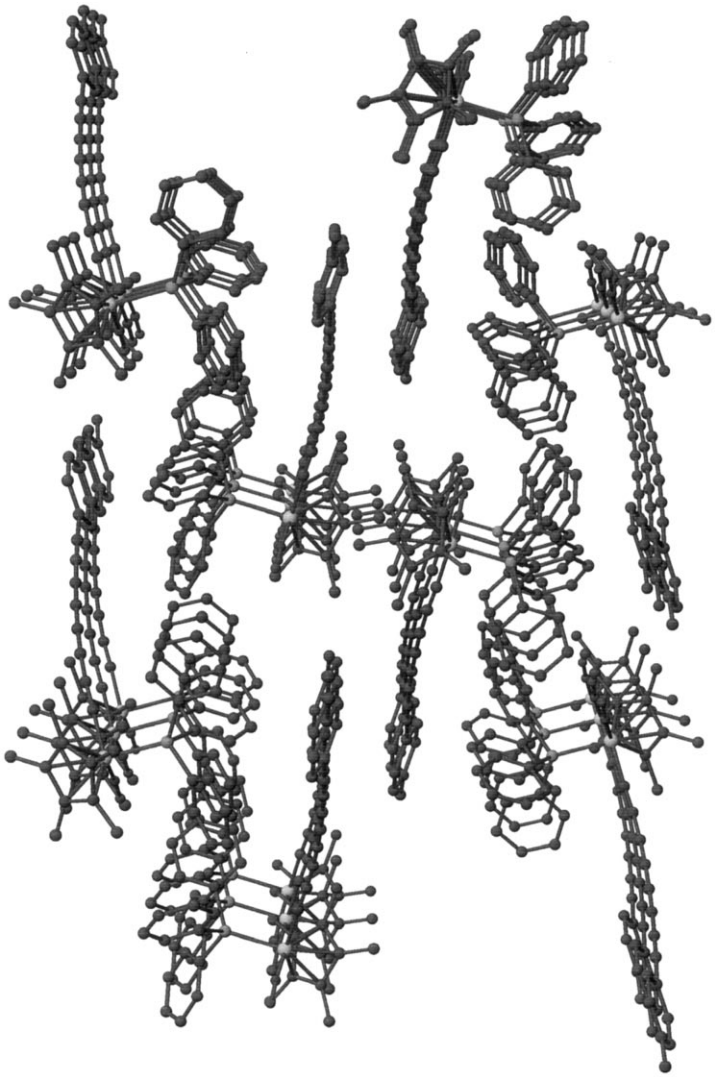

Fig. 6. Representative packing diagram for crystalline **8**.

(PPh_3)(C≡CH), which as analyzed earlier is even less acidic [17].

We can define no basis for sp carbon chain curvature in crystalline **7** and **8** other than packing forces. If this is indeed the dominant factor, then the lack of precedent among the compounds in Table 4 is surprising. Density functional calculations (B3LYP/6-31G*) on the model compound $CH_3C{\equiv}CC{\equiv}CC{\equiv}C$-*p*-$C_6H_4Me$ show that only 3–4 kcal mol^{-1} are required to produce the degree of bending in Fig. 3 [37]. Also, a search of the Cambridge crystallographic data base reveals ten structurally characterized triynes [38]. None of these show any appreciable bending. Hence, they are not discussed here, and interested readers are referred to a previous analysis of packing motifs in these compounds [38d]

The correlation of the site of protonation of **7** (Scheme 4) with the region of maximum chain curvature in the solid state is probably accidental. However, density functional calculations (B3LYP/LANL2DZ + p) on the model compound (η^5-C_5Me_5)Re(NO)(PMe_3)(C≡CC≡CC≡CH) suggest that protonation of the ≡CH terminus would give the most stable product [37]. This implicates another, non-thermodynamic, controlling feature. Regardless, the regiochemistry is somewhat unfortunate, as we had hoped to use these compounds as precursors to species with $^+$Re=(C=C)$_n$(X)(Ar) linkages. Using other synthetic approaches, we have been able to isolate labile complexes of the formula $^+$Re=C=C=C=C=C(Ar)$_2$ [39].

In summary, this study has provided the first demonstration that sp carbon chains can exhibit significant bending or curvature in the solid state. This constitutes important support for the conjecture that sp carbon chains might easily coil as they grow under various gas phase conditions, leading to intramolecular carbon–carbon bond formation and ultimately fullerenes. We will continue to structurally characterize all compounds with at least eight consecutive sp carbons that we are able to crystallize, and anticipate the serendipitous discovery of additional unusual bonding and packing motifs.

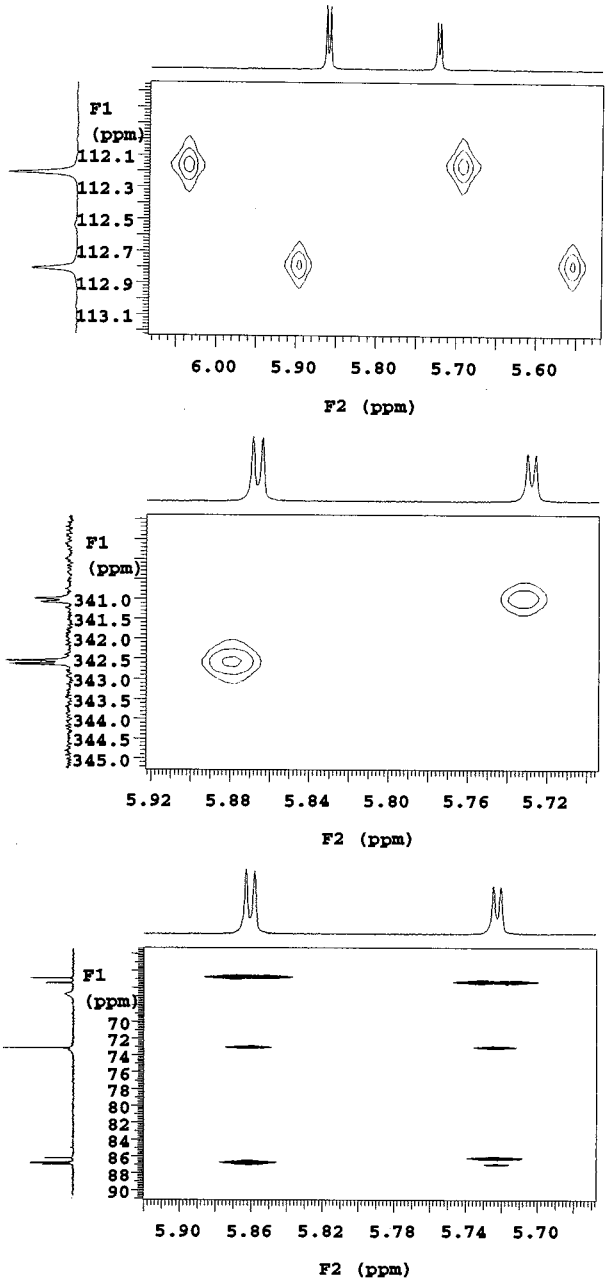

Fig. 7. A ^{1}H-^{13}C-HMQC spectrum of **9** (top) and ^{1}H-^{13}C-HMBC spectra of **9** (middle, bottom). The 1D reference spectra are derived from different samples.

4. Experimental

4.1. General data

Reactions were conducted under N_2 atmospheres. Commercial chemicals were treated as follows: acetone, distilled from anhydrous $CaSO_4$; THF, ether, benzene, hexanes, distilled from Na/benzophenone; toluene, distilled from Na; pyrrolidine, CH_2Cl_2/CD_2Cl_2, distilled/vacuum transferred from CaH_2; HC≡C-*p*-C_6H_4Me (Aldrich, Lancaster), $HC{\equiv}CSiEt_3$ (Farchan, GFS), $AgNO_3$ (Spectrum, 99 + %), NBS (Aldrich), *n*-$Bu_4N^+F^-$ (Aldrich, Lancaster; 1.0 M in THF/5 wt% H_2O), CuI (Aldrich, 99.999%), $EtNH_2$ (Aldrich, anhydrous; 99% or 2.0 M in THF), *t*-BuOK (Janssen), and silica gel (J.T. Baker, 60–200 mesh), used as received; *n*-BuLi (Acros, 2.5 M in hexane) [40] and $HBF_4{\cdot}OEt_2$ (Aldrich, two similar weight concentrations in ether: 54% HBF_4 or 85% $HBF_4{\cdot}OEt_2$) [41], standardized. Other materials not listed were used as received.

IR and UV–visible spectra were recorded on Mattson Polaris FT and Hewlett Packard 8452A spectrometers. 1D-NMR spectra were obtained on Varian 300 or 500 MHz spectrometers. Mass spectra were recorded on a Finnigan MAT 95 high resolution instrument. Differential scanning calorimetry (DSC) was conducted on a TA Instruments model 2910 equipped with software ('Universal Analysis') for T_i, T_e, and T_p values [42]. Samples (1–2 mg) were loaded in crimped Al pans and heated to 300°C at 5°C min^{-1} under N_2. Microanalyses were conducted by Atlantic Microlab.

4.2. BrC≡C-*p*-C_6H_4Me [15,16]

A flask was charged with HC≡C-*p*-C_6H_4Me (2.555 g, 22.00 mmol), $AgNO_3$ (1.308 g, 7.700 mmol) and acetone (20 ml). The mixture was stirred. After 20 min, acetone (100 ml) and NBS (3.920 g, 22.02 mmol) were added. After 12 h, ether (100 ml) was added. The mixture (and 2 × 10 ml ether rinses) were filtered. Ice water (40 ml) was poured onto the filtrate with stirring. The water layer was extracted with ether (2 × 20 ml). The combined ether layers were dried over Na_2SO_4. Solvents were removed by rotary evaporation at room temperature and the residue was vacuum transferred by oil pump vacuum to give BrC≡C-*p*-C_6H_4Me (3.076 g, 15.77 mmol, 72%) as a colorless liquid that was stored in a freezer. The IR and ^{1}H-NMR spectra matched those previously reported [15a].

IR (cm^{-1}, CH_2Cl_2) $\nu_{C\equiv C}$ 2201 vs. NMR: ^{1}H (δ, $CDCl_3$, 300 MHz) 7.32 (d, $J_{HH} = 8.1$ Hz, 2H of C_6H_4), 7.09 (d, $J_{HH} = 8.1$ Hz, 2H of C_6H_4), 2.33 (s, CH_3); $^{13}C\{^{1}H\}$ (ppm, $CDCl_3$, 126 MHz) [43] 139.0 (s, *i* to $C_6H_4CH_3$), 132.0 (s, *m* to $C_6H_4CH_3$), 129.2 (s, *o* to $C_6H_4CH_3$), 119.7 (s, *p* to $C_6H_4CH_3$), 80.3 (s, $\underline{C}{\equiv}CBr$), 49.0 (s, $C{\equiv}\underline{C}Br$), 21.6 (s, CH_3).

4.3. BrC≡C$SiEt_3$ [16,21]

The compounds $HC{\equiv}CSiEt_3$ (1.263 g, 9.000 mmol), $AgNO_3$ (0.380 g, 2.24 mmol), acetone (100 ml), and NBS (1.869 g, 10.50 mmol) were combined in a procedure analogous to that given for BrC≡C-*p*-C_6H_4Me. An identical workup gave $BrC{\equiv}CSiEt_3$ as a colorless liquid (1.406 g, 6.988 mmol, 78%).

IR (cm^{-1}, film/CH_2Cl_2) $\nu_{C\equiv C}$ 2123/2120 vs. NMR: ^{1}H (δ, C_6D_6, 300 MHz) 0.96 (t, $J_{HH} = 7.8$ Hz, CH_2),

0.52 (q, $J_{HH} = 7.8$ Hz, CH_3); $^{13}C\{^1H\}$ (ppm, C_6D_6, 75 MHz) 84.9 (s, $\underline{C}\equiv CBr$), 62.8 (s, $C\equiv\underline{C}Br$), 7.6 (s, CH_2), 4.7 (s, CH_3).

4.4. (η^5-C_5Me_5)Re(NO)(PPh_3)(C≡CC≡CH) (2) [17]

A flask was charged with (η^5-C_5Me_5)Re(NO)(PPh_3)(C≡CC≡CSiMe_3) (**1a**; [17] 0.162 g, 0.220 mmol) and THF (20 ml). Then *n*-$Bu_4N^+F^-$ (1.0 M in THF/5 wt% H_2O; 0.044 ml, 0.044 mmol) was added dropwise with stirring. After 0.5 h, the mixture was filtered through a 1 cm silica gel pad. Solvent was removed from the red filtrate by oil pump vacuum. The residue was dissolved in a minimum of benzene (ca. 3 ml), and hexane (50 ml) was added. The sample was kept at −20°C (freezer, 16 h). Dark red–orange microcrystals of **2** were isolated by filtration and dried by oil pump vacuum (0.133 g, 0.201 mmol, 91%). The IR and NMR spectra matched those previously reported [17].

4.5. (η^5-C_5Me_5)Re(NO)(PPh_3)(C≡CC≡CC≡CSiMe_3) (3a)

(**A**) A Schlenk flask was charged with **2** (0.0900 g, 0.136 mmol), CuI (0.0285 g, 0.150 mmol), and THF (10 ml), and cooled to −45°C (CO_2/CH_3CN). Then *n*-BuLi (2.2 M in hexane; 0.093 ml, 0.20 mmol) was added with stirring. After 15 min, $EtNH_2$ (ca. 0.6 ml) and a solution of IC≡CSiMe_3 [20] (0.0403 g, 0.136 mmol) in THF (1 ml; dropwise over 15 min) were added. The cold bath was removed. After 10 min, solvent was removed by rotary evaporation. The residue was extracted with toluene (3 × 8 ml). The extracts were filtered through a 1 cm silica gel pad, which was washed with toluene (2 × 10 ml). Solvent was removed from the red filtrate by rotary evaporation. The residue was dissolved in a minimum of THF (ca. 2 ml), and hexane/THF (5 ml, 3:1 v/v) was added. The solution was chromatographed on a silica gel column (20 × 2 cm; 1:1 v/v hexane/THF). Solvent was removed from a red fraction by oil pump vacuum. The orange–red solid was dissolved in a minimum of THF (ca. 1 ml) and hexane (15 ml) was added. The sample was kept at −90°C (4 h). The supernatant was decanted to give **3a** as an orange powder that was dried by oil pump vacuum (0.0496 g, 0.0653 mmol, 48%). Anal. Calc. for $C_{37}H_{39}NOPReSi$: C, 58.55; H, 5.18. Found: C, 58.48; H, 5.34. (**B**) A Schlenk flask was charged with **2** (0.0292 g, 0.0437 mmol), THF (10 ml), IC≡CSiMe_3 (0.0110 g, 0.0372 mmol) and pyrrolidine (0.117 g, 1.65 mmol). Then CuI (0.0003 g, 0.0013 mmol) was added with stirring. After 40 min, solvent was removed by oil pump vacuum. The residue was dissolved in a minimum of THF (ca. 2 ml), and hexane/THF was added (3:1 v/v, ca. 5 ml). The mixture was chromatographed on a silica gel column (10 × 2 cm; 1:1 v/v hexane/THF). Two red bands were collected separately, and solvents were removed by rotary evaporation. The second residue was **2** (0.0012 g, 0.0018 mmol, 4%). The first was dissolved in a minimum amount THF (ca 1 ml), and hexane (ca. 15 ml) was added. The sample was kept at −90°C (4 h). Solvent was decanted from an orange powder that was dried by oil pump vacuum to give **3a** (0.0125 g, 0.0165 mmol, 44%). (**C**) A Schlenk flask was charged with **2** (0.066 g, 0.10 mmol) and THF (5 ml), and cooled to −45°C. Then *n*-BuLi (2.2 M in hexane, 50 ml, 0.11 mmol) and (after 2 h) solid [PhIC≡CSiMe_3]$^+$TfO$^-$ (0.045 g, 0.10 mmol) [23] were added with stirring. After 1 h, the cold bath was removed. After 0.5 h, solvent was removed by oil pump vacuum. The residue was extracted with toluene (2 × 5 ml). The extract was filtered through a 2 cm silica gel pad. Solvent was removed from the filtrate by oil pump vacuum. The residue was extracted with boiling hexane (2 × 100 ml). The extract was filtered and kept at −90°C (24 h). Red–brown microcrystals were isolated by filtration and dried by oil pump vacuum to give **3a** (0.038 g, 0.050 mmol, 50%), m.p. (dec.) 185–188°C $R_f = 0.68$ [44b].

IR (cm^{-1}, THF) $\nu_{C\equiv C}$ 2132 m, 2109 m, 1979 vs., ν_{NO} 1656 vs. NMR: ^1H (δ, CD_2Cl_2/C_6D_6, 300 MHz) 7.54–7.40/7.70–7.61 + 7.05–6.88 (m, 15H/6 + 9H, $3C_6H_5$), 1.74/1.52 (s, $C_5(CH_3)_5$), 0.17/0.39 (s, $SiMe_3$); $^{13}C\{^1H\}$ (ppm, C_6D_6, 75 MHz) 135.2 (d, $J_{CP} = 54.5$, *i*-Ph), 134.6 (d, $J_{CP} = 10.2$ Hz, *o*-Ph), 130.7 (s, *p*-Ph), 128.7 (*m*-Ph) [45], 113.3 (d, $J_{CP} = 15.9$ Hz, Re$\underline{C}\equiv$), 112.8 (s, ReC≡$\underline{C}$), 101.3 (s, $\underline{C}_5(CH_3)_5$), 92.2, 86.3 (2 s, $\underline{C}\equiv\underline{C}$Si), 66.5, 63.8 (2 s, ReC≡C$\underline{C}\equiv\underline{C}$), 10.3 (s, $C_5(\underline{C}H_3)_5$), 0.5 (s, $SiCH_3$); $^{31}P\{^1H\}$ (ppm, CD_2Cl_2/C_6D_6, 121 MHz) 23.3/19.7 (s). UV–vis (8.7×10^{-5} M) [46] 236 (21700), 268 sh (13600), 288 sh (14600), 300 sh (16000), 312 (17800), 380 sh (6000), 410 sh (4400). MS (positive FAB, 3-NBA/THF) [47] 759 (M^+, 100%), 614 ((η^5-C_5Me_5)Re(NO)(PPh_3)$^+$, 36%); no other peaks above 300 of > 10%.

4.6. (η^5-C_5Me_5)Re(NO)(PPh_3)(C≡CC≡CC≡CSiEt_3) (3b)

(**A**) A Schlenk flask was charged with **2** (0.250 g, 0.378 mmol), *t*-BuOCu [25] (0.052 g, 0.38 mmol), and THF (50 ml). The mixture was stirred for 2 h and cooled to −20°C. Then $EtNH_2$ (0.4 ml) and a solution of BrC≡CSiEt_3 (0.0829 g, 0.378 mmol) in THF (0.5 ml; dropwise over 15 min) were added. The cold bath was removed. After 0.5 h, solvent was removed by rotary evaporation. The residue was extracted with toluene (3 × 10 ml). The extract was filtered through a 7 cm silica gel pad. Solvent was removed from the filtrate by oil pump vacuum. The residue was dissolved in a minimum of THF (ca. 2 ml), and hexane was added (5 ml). The solution was chromatographed on a silica gel column (10 × 2 cm; 3:1 v/v hexane/THF). Solvent was

removed from a red fraction by oil pump vacuum. The red–brown solid was extracted with hot hexane (15 ml). The extract was filtered and kept in a −90°C freezer (16 h). Red microcrystals of **3b** were isolated by filtration at −80°C (CO_2/acetone) and dried by oil pump vacuum (0.196 g, 0.245 mmol, 65%). (**B**) A Schlenk flask was charged with **2** (1.620 g, 2.204 mmol), CuI (0.4407 g, 2.314 mmol), and THF (150 ml), and cooled to −45°C (CO_2/CH_3CN). Then *n*-BuLi (2.0 M in hexane; 1.2 ml, 2.3 mmol) was added with stirring. After 45 min, $EtNH_2$ (ca. 1.5 ml) and a solution of $BrC{\equiv}CSiEt_3$ (0.5068 g, 2.314 mmol) in THF (5 ml; dropwise over 15 min) were added. The cold bath was removed. After 10 min, solvent was removed by rotary evaporation. The residue was extracted with benzene (3 × 8 ml). The extract was filtered through a 2 cm silica gel pad, which was washed with benzene (2 × 10 ml). Solvent was removed from the filtrate by oil pump vacuum. The residue was dissolved in a minimum of benzene (ca. 5 ml), and chromatographed on a silica gel column (25 × 5 cm; benzene). Solvent was removed from a red fraction by oil pump vacuum. The red–brown solid was dissolved in hot hexane (50 ml), and red microcrystals of **3b** were obtained as in procedure **A** (1.478 g, 1.845 mmol, 84%), m.p. 182°C. $R_f = 0.73$ [44b]. Anal. Calc. for $C_{40}H_{45}NOPReSi$: C, 59.98; H, 5.66. Found: C, 60.01; H, 5.66.

IR (cm^{-1}, THF) $\nu_{C\equiv C}$ 2132 m, 2110 m, 1979 vs., ν_{NO} 1658 vs. NMR: ^1H (δ, C_6D_6, 300 MHz) 7.71–7.59 (m, 6H of $3C_6H_5$), 7.06–6.92 (m, 9H of $3C_6H_5$), 1.52 (s, $C_5(CH_3)_5$), 0.99 (t, $J_{HH} = 8.1$ Hz, $3CH_2C\underline{H}_3$), 0.55 (q, $J_{HH} = 8.1$ Hz, $3SiCH_2$); $^{13}C\{^1H\}$ (ppm, C_6D_6, 75 MHz) 134.9 (d, $J_{CP} = 51.6$ Hz, *i*-Ph), 134.2 (d, $J_{CP} = 10.5$ Hz, *o*-Ph), 130.3 (s, *p*-Ph), 128.5 (*m*-Ph) [45], 112.5 (s, $ReC{\equiv}\underline{C}$), 112.3 (d, $J_{CP} = 16.4$ Hz, $Re\underline{C}{\equiv}C$), 100.0 (s, $\underline{C}_5(CH_3)_5$), 92.7, 83.7 (2 s $\underline{C}{\equiv}\underline{C}Si$), 65.4 (d, $J_{CP} = 3.6$ Hz, $ReC{\equiv}C\underline{C}$), 63.6 (s, $\underline{C}C{\equiv}CSi$), 9.8 (s, $C_5(\underline{C}H_3)_5$), 7.7 (s, $SiCH_2\underline{C}H_3$), 4.9 (s, $Si\underline{C}H_2$); $^{31}P\{^1H\}$ (ppm, C_6D_6/THF, 121 MHz) 20.5/20.9 (s). UV–vis (1.7×10^{-5} M) [46] 234 (92400), 266 (54800), 288 sh (65100), 312 (88100), 370 (15300), 408 (7000). MS (EI, 30 eV) [47] 801 (M^+, 43%), 262 (PPh_3^+, 100%); no other peaks above 200 of >5%.

4.7. (η^5-C_5Me_5)Re(NO)(PPh_3)(C≡CC≡CC≡CH) (5)

(**A**) Complex **3b** (0.0980 g, 0.122 mmol), *n*-$Bu_4N^+F^-$ (1.0 M in THF/5 wt% H_2O; 0.036 ml, 0.036 mmol), and THF (20 ml) were combined in a procedure analogous to that given for **2**. An identical workup gave **5** as a red powder (0.0738 g, 0.107 mmol, 88%). (**B**) A Schlenk flask was charged with **3b** (0.040 g, 0.050 mmol), freshly ground K_2CO_3 (0.007 g, 0.05 mmol), and MeOH (5 ml). The mixture was stirred vigorously. After 24 h, solvent was removed by oil pump vacuum. The residue was extracted with THF (2 × 3 ml). The extract was filtered through a 1 cm Celite pad. Solvent was removed from the red filtrate by oil pump vacuum. The residue was dissolved in minimum of THF, and hexane (10 ml) was added. Solvent was removed by oil pump vacuum to give **5** as a reddish brown powder (0.036 g, 0.045 mmol, 90%), m.p. (dec.) 160–165°C. Anal. Calc. for $C_{34}H_{31}NOPRe$: C, 59.46; H, 4.55. Found: C, 59.46; H, 4.60.

IR (cm^{-1}, THF) $\nu_{C\equiv C}$ 2140 s, 2080 m, 1970 m, ν_{NO} 1658 vs. NMR: ^1H (δ, C_6D_6, 300 MHz) 7.69–7.62 (m, 6H of $3C_6H_5$), 7.05–6.88 (m, 9H of $3C_6H_5$), 1.69 (s, ≡CH), 1.52 (s, $C_5(CH_3)_5$); $^{13}C\{^1H\}$ (ppm, CD_2Cl_2, 75 MHz) 135.0 (*i*-Ph) [45], 134.3 (d, $J_{CP} = 10.7$ Hz, *o*-Ph), 130.8 (s, *p*-Ph), 128.7 (d, $J_{CP} = 10.3$ Hz, *m*-Ph), 113.6 (d, $J_{CP} = 15.4$ Hz, $Re\underline{C}{\equiv}C$), 111.2 (s, $ReC{\equiv}\underline{C}$), 101.7 (s, $\underline{C}_5(CH_3)_5$), 70.3 (s, $\underline{C}{\equiv}CH$), 68.4 (s, ≡CH), 63.7 (d, $J_{CP} = 2.8$ Hz, $ReC{\equiv}C\underline{C}$), 61.5 (s, $\underline{C}C{\equiv}CH$), 10.3 (s, $C_5(\underline{C}H_3)_5$); $^{31}P\{^1H\}$ (ppm, toluene, 121 MHz) 21.0 (s). UV–vis (2.9×10^{-5} M) [46] 266 sh (28400), 282 sh (33300), 304 (35100), 360 (7800), 394 (4000). MS (positive FAB, 3-NBA/CH_2Cl_2) [47] 687 (M^+, 100%), 614 ((η^5-C_5Me_5)Re(NO)(PPh_3)$^+$, 14%); no other peaks above 400 of >10%.

4.8. (η^5-C_5Me_5)Re(NO)(PPh_3)(C≡CC≡CC≡C-*p*-C_6H_4Me) (7)

(**A**) A Schlenk flask was charged with **2** (0.508 g, 0.767 mmol), CuI (0.146 g, 0.767 mmol), and THF (50 ml), and cooled to −45°C (CO_2/CH_3CN). Then *n*-BuLi (2.2 M in hexane; 0.35 ml, 0.77 mmol) was added with stirring. After 20 min the mixture was transferred to a −20°C bath. Then $EtNH_2$ (ca. 1.0 ml) and a solution of freshly distilled $BrC{\equiv}C$-*p*-C_6H_4Me (0.150 g, 0.767 mmol) in THF (5 ml; dropwise over 15 min) were added. After 10 min, the cold bath was removed. Solvent was removed by rotary evaporation. The residue was extracted with benzene (3 × 15 ml). The extract was filtered through a 2 cm silica gel pad. Solvent was removed from the bright red–orange filtrate by oil pump vacuum. The residue was chromatographed on a silica gel column (15 × 2 cm; 2:1 v/v hexane/THF). Solvent was removed from a red fraction by oil pump vacuum. The residue was dissolved in a minimum of toluene (ca. 1.5 ml), and hexane was added (20 ml). The mixture was kept at −90°C (16 h). Dark red crystals of **7** were collected by filtration at −80°C and dried by oil pump vacuum (0.459 g, 0.591 mmol, 77%). (**B**) A Schlenk flask was charged in an inert atmosphere box with **1a** (0.250 g, 0.341 mmol), *t*-BuOCu (0.061 g, 0.44 mmol) and THF (50 ml). Then *n*-$Bu_4N^+F^-$ (1.0 M in THF/5 wt% H_2O, 0.068 ml, 0.068 mmol) was added with stirring. After 1.5 h, an IR spectrum showed the absence of **1a** and **2** [19]. The mixture was cooled to −20°C. Then $EtNH_2$ (ca. 0.7

ml) and a solution of BrC≡C-*p*-C_6H_4Me (0.066 g, 0.34 mmol) in THF (5 ml; dropwise over 15 min) were added. After 0.5 h, solvent was removed by rotary evaporation. The residue was extracted with benzene (3 × 15 ml). The extract was filtered through a 2 cm silica gel pad. Solvent was removed from the filtrate by rotary evaporation. The residue was chromatographed on a silica gel column (25 × 2 cm; 3:1 v/v hexane/THF). Solvent was removed from a red fraction by oil pump vacuum. The residue was dissolved in a minimum of toluene (ca. 3 ml), and hexane (30 ml) was added. The mixture was kept at −90°C (16 h) and **7** was collected as above (0.215 g, 0.277 mmol, 81%). DSC ($T_i/T_e/T_p$) [42] 170/193/211°C. Anal. Calc. for $C_{41}H_{37}NOPRe$: C, 63.38; H, 4.80. Found: C, 63.30; H, 4.64. $R_f = 0.70$ [44a]/0.59 [44b].

IR (cm^{-1}, THF) $\nu_{C\equiv C}$ 2161 w, 2114 vs., 1997 m, ν_{NO} 1650 vs. NMR: ^1H (δ, CD_2Cl_2/C_6D_6, 500/300 MHz) 7.55–7.48/7.74–7.66 (m, 6H of $3C_6H_5$), 7.46–7.42/7.07–6.93 (m, 9H of $3C_6H_5$), 7.32/7.23 (d, $^3J_{HH} = 8.3/8.0$ Hz, 2H of *m* to $C_6H_4\mathbf{C}H_3$), 7.12/6.63 (d, $^3J_{HH} = 7.8/8.0$ Hz, 2H of *o* to $C_6H_4\mathbf{C}H_3$), 2.35/1.91 (s, 3H, CH_3), 1.76/1.52 (s, 15H, $C_5(CH_3)_5$); $^{13}C\{^1H\}$ (ppm, CD_2Cl_2, 126 MHz) 139.4 (s, *i* to $C_6H_4\mathbf{C}H_3$) [43], 135.2 (s, *i*-PPh) [45], 134.4 (d, $J_{CP} = 10.5$ Hz, *o*-PPh), 133.0 (s, *m* to $C_6H_4\mathbf{C}H_3$) [43], 130.9 (s, *p*-PPh), 129.6 (s, *o* to $C_6H_4\mathbf{C}H_3$) [43], 128.8 (d, $J_{CP} = 10.5$ Hz, *m*-PPh), 119.9 (s, *p* to $C_6H_4\mathbf{C}H_3$) [43], 115.8 (d, $J_{CP} = 16.2$ Hz, Re$\underline{C}$≡C), 111.8 (s, ReC≡$\underline{C}$), 101.8 (s, $\underline{C}_5(CH_3)_5$), 78.2, 75.5 (2 s, $\underline{C}$≡$\underline{C}$-*p*-C_6H_4Me), 70.0 (d, $J_{CP} = 3.2$ Hz, ReC≡C$\underline{C}$), 61.4 (s, ReC≡CC≡$\underline{C}$), 21.8 (s, $C_6H_5\underline{C}H_3$), 10.3 (s, $C_5(\underline{C}H_3)_5$); $^{31}P\{^1H\}$ (ppm, C_6D_6, 121 MHz) 20.6 (s). UV–vis (1.4×10^{-5} M) [46] 232 (52000), 260 sh (42000), 274 (43000), 302 sh (44000), 320 (67000), 358 sh (23000), 388 sh (15000), 416 sh (9500). MS (positive FAB, 3-NBA/THF) [47] 777 (M^+, 100%), 614 ($(\eta^5\text{-}C_5Me_5)Re(NO)(PPh_3)^+$, 40%); no other peaks above 400 of >15%.

4.9. (η^5-C_5Me_5)Re(NO)(PPh_3)(C≡CC≡CC≡CC≡C-*p*-C_6H_4Me) (**8**)

(**A**) A Schlenk flask was charged with **5** (0.2840 g, 0.4134 mmol), CuI (0.0827 g, 0.4341 mmol) and THF (50 ml), and cooled to −45°C. Then *n*-BuLi (2.4 M in hexane; 0.18 ml, 0.43 mmol) was added with stirring. After 25 min the mixture was transferred to a −20°C bath. Then $EtNH_2$ (ca. 0.5 ml) and a solution of BrC≡C-*p*-C_6H_4Me (0.0847 g, 0.4341 mmol) in THF (5 ml; dropwise over 15 min) were added. The cold bath was removed. After 10 min, solvent was removed by rotary evaporation. The residue was extracted with benzene (3 × 8 ml). The extract was filtered through a 2 cm silica gel pad, which was washed with benzene (2 × 5 ml). Solvent was removed from the filtrate by oil pump vacuum. The residue was dissolved in a minimum of benzene (ca. 3 ml) and passed through a silica gel column (15 × 2 cm, benzene). A red band was collected, concentrated by rotary evaporation, and chromatographed on a silica gel column (30 × 2 cm; 2:1 v/v hexane/THF). Solvent was removed from a red fraction by oil pump vacuum to give **8** as a reddish–brown powder (0.2187 g, 0.2731 mmol, 66%). (**B**) A Schlenk flask was charged with **3b** (0.141 g, 0.176 mmol) and THF (40 ml). Then *n*-$Bu_4N^+F^-$ (1.0 M in THF/5 wt% H_2O, 0.053 ml, 0.053 mmol) was added with stirring. After 0.5 h, *t*-BuOCu (0.036 g, 0.26 mmol) was added and the mixture was stirred for 2 h. The mixture was cooled to −20°C. Then $EtNH_2$ (ca 0.7 ml) and a solution of BrC≡C-*p*-C_6H_4Me (0.034 g, 0.18 mmol) in THF (1.5 ml; dropwise over 15 min) were added. After 10 min, the cold bath was removed. Solvent was removed by rotary evaporation. The residue was extracted with benzene (3 × 15 ml). The extract was filtered through a 2 cm silica gel pad. Solvent was removed from the filtrate by rotary evaporation. The residue was chromatographed on a silica gel column (20 × 2 cm; 3:1 v/v hexane/THF). Solvent was removed from a red fraction by oil pump vacuum. The residue was dissolved in a minimum of toluene (ca. 3 ml), and hexane (50 ml) was added. The mixture was kept at −90°C (16 h). A dark red powder was collected by filtration at −80°C and dried by oil pump vacuum to give **8** (0.101 g, 0.125 mmol, 71%). (**C**) A Schlenk flask was charged with **3b** (0.136 g, 0.170 mmol) and THF (20 ml). Then *n*-$Bu_4N^+F^-$ (1.0 M in THF/5 wt% H_2O, 0.051 ml, 0.051 mmol) was added with stirring. After 0.5 h, an IR spectrum showed that **3b** had been consumed. Then CuI (0.0323 g, 0.170 mmol) and *t*-BuOK (0.0210 g, 0.187 mmol) were added. The mixture was stirred (1 h) and cooled to −60°C (acetone partially cooled by CO_2). Then $EtNH_2$ (ca 0.5 ml) and a solution of BrC≡C-*p*-C_6H_4Me (0.0331 g, 0.170 mmol) in THF (1.5 ml; dropwise over 15 min) were added. After 0.5 h, solvent was removed by oil pump vacuum. The residue was extracted with toluene (3 × 5 ml). The extract was filtered through a 2 cm silica gel pad. Solvent was removed from the filtrate by rotary evaporation. Column chromatography on silica gel (30 × 2 cm; 3:1 v/v hexane/THF) gave two red bands that were collected separately. Solvents were removed by oil pump vacuum to give **8** as a reddish–brown powder (0.0686 g, 0.0857 mmol, 50%) and (η^5-C_5Me_5)Re(NO)(PPh_3)(C≡C)$_6$(Ph_3P)(ON)Re(η^5-C_5Me_5) (0.0160 g, 0.0117 mmol, 14%) [12b,c]. Dark red microcrystals of **8** were obtained from CH_2Cl_2/hexane (−20°C). DSC ($T_i/T_e/T_p$) [42] 162/181/204°C. $R_f = 0.76$ [44a]. Anal. Calc. for $C_{43}H_{37}NOPRe$: C, 64.48; H, 4.66. Found: C, 64.26; H, 5.06.

IR (cm^{-1}, THF) $\nu_{C\equiv C}$ 2180 w, 2119 w, 2070 vs., 1975 s, ν_{NO} 1659 s. NMR: ^1H (δ, CD_2Cl_2, 300 MHz) 7.54–7.41 (m, 15H of $3C_6H_5$), 7.38 (d, $^3J_{HH} = 8.1$ Hz, 2H *m*

to $C_6H_4CH_3$), 7.14 (d, $^3J_{HH} = 8.1$ Hz, 2H *o* to $C_6H_4CH_3$), 2.36 (s, 3H, CH_3), 1.75 (s, 15H, $C_5(CH_3)_5$); $^{13}C\{^1H\}$ (ppm, CD_2Cl_2, 126 MHz) 140.5 (s, *i* to $C_6H_4CH_3$) [43], 134.8 (s, *i*-PPh) [45], 134.4 (d, $J_{CP} =$ 10.7 Hz, *o*-PPh), 133.4 (s, *m* to $C_6H_4CH_3$) [43], 131.0 (s, *p*-PPh), 129.8 (s, *o* to $C_6H_4CH_3$) [43], 128.9 (d, $J_{CP} =$ 10.7 Hz, *m*-PPh), 119.9 (d, $J_{CP} = 15.1$ Hz, Re$\underline{C}$≡C), 118.9 (s, *p* to $C_6H_4CH_3$) [43], 112.4 (s, ReC≡$\underline{C}$), 102.1 (s, $\underline{C}_5(CH_3)_5$), 78.0, 74.9 (2 s, $\underline{C}$≡$\underline{C}$-*p*-C_6H_4Me), 67.4 (d, $J_{CP} = 2.4$ Hz, ReC≡C$\underline{C}$), 68.3, 63.9, 63.3 (3 s, ReC≡CC≡$\underline{CC}$≡$\underline{C}$), 21.9 (s, $C_6H_5\underline{C}H_3$), 10.3 (s, $C_5(\underline{C}H_3)_5$); $^{31}P\{^1H\}$ (ppm, CD_2Cl_2, 121 MHz) 19.6 (s). UV–vis (7.5×10^{-6} M) [46] 232 (56000), 270 (48000), 282 (49000), 294 (49000), 314 (43000), 336 sh (62000), 356 (89000), 404 sh (17000), 432 sh (12000), 472 sh (8500). MS (positive FAB, 3-NBA/THF) [47] 801 (M^+, 100%), 614 ($(\eta^5\text{-}C_5Me_5)Re(NO)(PPh_3)^+$, 15%); no other peaks above 400 of > 3%.

4.10. $[(\eta^5\text{-}C_5Me_5)Re(NO)(PPh_3)(C{=}C(H)C{\equiv}CC{\equiv}C\text{-}p\text{-}C_6H_4Me)]^+ BF_4^-$ (9)

(**A**) A 5 mm NMR tube was charged with **7** (0.0069 g, 0.0089 mmol) and CD_2Cl_2 (0.70 ml), capped with a septum, and cooled in liquid N_2. Then $HBF_4{\cdot}OEt_2$ (7.0 M in ether; 1.4 μl, 0.0095 mmol) was added via syringe. The tube was placed in a −95°C bath (liq. N_2/toluene), shaken, and quickly transferred to a −80°C NMR probe. Data: see text. (**B**) A Schlenk flask was charged with **7** (0.0570 g, 0.0732 mmol), CH_2Cl_2 (2 ml), and ether (10 ml), and cooled to −80°C (CO_2/acetone). Then $HBF_4{\cdot}OEt_2$ (5.78 M in ether; 0.013 ml, 0.073 mmol) was added with stirring. After 10 min, the cold bath was removed. After 0.5 h, solvent was removed by oil pump vacuum. Ether (10 ml) was added. The yellow powder was collected by filtration, washed with ether (3×2 ml), and dried by oil pump vacuum to give **9** (0.0534 g, 0.0618 mmol, 84%) as (60 ± 2):(40 ± 2) mixture of *ac*/*sc* Re=C=C isomers. Crystallization attempts involving CH_2Cl_2 and ether or hydrocarbons were complicated by the competing slow decomposition of **9**.

IR (cm^{-1}): KBr, $\nu_{C\equiv C}$ 2204 w, 2106 w, $\nu_{C=C}$ 1647 m, ν_{NO} 1715 s; CH_2Cl_2, $\nu_{C\equiv C}$ 2212 w, 2206 w, 2110 w, 2106 w, ν_{NO} 1734 vs. NMR, *ac*-**9**: ^1H (δ, CD_2Cl_2, 500 MHz) 7.68–7.16 (m, $3C_6H_5$, C_6H_4), 5.88 (d, $J_{HP} = 2.39$ Hz, Re=C=CH), 2.38 (s, $C_6H_4C\underline{H}_3$), 1.98 (s, $C_5(CH_3)_5$); $^{13}C\{^1H\}$ (ppm, CD_2Cl_2, 126 MHz; see also Chart 1) 342.7 (d, $J_{CP} = 10.4$ Hz, Re=$\underline{C}$=C), 141.1 (s, *i* to $C_6H_4CH_3$) [43], 133.9 (d, $J_{CP} = 12.1$ Hz, *o*-PPh), 133.40 (s, *m* to $C_6H_4CH_3$) [43], 133.23 (s, *p*-PPh), 132.7 (s, *o* to $C_6H_4CH_3$) [43], 130.16 (d, $J_{CP} = 11.3$ Hz, *m*-PPh), 118.4 (s, *p* to $C_6H_4CH_3$) [43], 112.2 (d, $J_{CP} = 4.0$ Hz, Re=C=$\underline{C}$), 111.0 (s, $\underline{C}_5(CH_3)_5$), 87.02 (s, C≡$\underline{C}$-*p*-C_6H_4Me), 86.9 (s, Re=C=CC≡$\underline{C}$), 73.2 (s, $\underline{C}$≡C-*p*-C_6H_4Me), 64.8 (s, Re=C=C$\underline{C}$), 21.9 (s, $C_6H_4\underline{C}H_3$), 10.4 (s, $C_5(\underline{C}H_3)_5$); $^{31}P\{^1H\}$ (ppm, CD_2Cl_2, 121 MHz) 22.9 (s). NMR, *sc* -**9**: ^1H (δ, CD_2Cl_2, 500 MHz) 7.68–7.16 (m, $3C_6H_5$, C_6H_4), 5.73 (d, $J_{HP} = 2.04$ Hz, Re=C=CH), 2.40 (s, $C_6H_4C\underline{H}_3$), 2.03 (s, $C_5(CH_3)_5$); $^{13}C\{^1H\}$ (ppm, CD_2Cl_2, 126 MHz; see also Chart 1) 341.1 (d, $J_{CP} =$ 10.8 Hz, Re=$\underline{C}$=C), 141.3 (s, *i* to $C_6H_4CH_3$) [43], 133.6 (d, $J_{CP} = 12.1$ Hz, *o*-PPh), 133.38 (s, *m* to $C_6H_4CH_3$) [43], 133.21 (s, *p*-PPh), 132.9 (s, *o* to $C_6H_4CH_3$) [43], 130.25 (d, $J_{CP} = 10.5$ Hz, *m*-PPh), 118.3 (s, *p* to $C_6H_4CH_3$) [43], 112.8 (d, $J_{CP} = 3.2$ Hz, Re=C=$\underline{C}$), 111.5 (s, $\underline{C}_5(CH_3)_5$), 87.15 (s, C≡$\underline{C}$-*p*-C_6H_4Me), 86.3 (s, Re=C=CC≡$\underline{C}$), 73.2 (s, $\underline{C}$≡C-*p*-C_6H_4Me), 65.4 (s, Re=C=C$\underline{C}$), 22.0 (s, $C_6H_4\underline{C}H_3$), 10.6 (s, $C_5(\underline{C}H_3)_5$); $^{31}P\{^1H\}$ (ppm, CD_2Cl_2, 121 MHz) 23.1 (s).

4.11. 2D NMR spectra

Data were obtained on a Varian Unity Inova 500 MHz spectrometer without sample spinning. The HMQC and HMBC data (Fig. 7) were acquired using a 5 mm indirect detection probe and the standard Varian pulse sequence (26°C; hypercomplex data matrix, 2048×2048 points with 16 transients time averaged per FID; spectral widths, 5071 and 18 492.8 Hz (^1H and ^{13}C dimensions); 90° pulse widths, 5.5 and 27.5 μs (^1H and ^{13}C channels)). ^{13}C broadband decoupling was not employed. Thus, the ^1H dimension of the top spectrum exhibits J_{CH}. Delays of 0.9 (relaxation) and 0.3 s (for suppressing signals from protons not bound to ^{13}C) were used. The J_{CH} parameter associated with the bird pulse was set to 140 Hz. The time domain data were zero filled to a 4096×4096 hypercomplex and multiplied by half-Gaussian functions of widths of 0.185 (^1H dimension) and 0.053 s (^{13}C dimension). Identical parameters and processing were used for HMBC data, except that the suppression time was set to zero, the bird pulse was suppressed, and the multibond evolution time between the ^1H 90° and 180° pulses was set to 55 ms, corresponding to a long-range coupling of 9 Hz. The 2D-INADEQUATE data (Chart 1) were acquired using a 0.28 M CD_2Cl_2 solution of **9** (−90°C), and a standard 5 mm broadband probe and Varian pulse sequence (inadqt), with maximum sensitivity set for $J_{CC} = 150$ Hz (hypercomplex data matrix, $16\,384 \times 256$ points (chemical shift and double-quantum dimensions) with 1024 transients time averaged per FID; spectral widths, $19\,323.7 \times 19\,323.7$ Hz; 90° pulse width, 16.5 μs; no relaxation delay). Proton decoupling was achieved using WALTZ modulation with a 101 μs 90° pulse. The data were analyzed using the NMRanalyst (FRED, Varian NMR Instruments) software package [35].

4.12. Crystallography

Dark red prisms of **7** were obtained by the slow evaporation of a CH_2Cl_2 solution (30 days). Prisms were later grown from CH_2Cl_2/hexane (vapor diffusion,

2 days), but it was not confirmed whether they were identical to those characterized crystallographically. Deep red orthogonal prisms of **8** were obtained from CH_2Cl_2/hexane (vapor diffusion, 5 days). Data were collected as outlined in Table 1 using a KUMA KM4 four-circle diffractometer with an Oxford Cryosystem–Cryostream cooler. Preliminary data for **8** were obtained from Weissenberg photographs (299(1) K: $a = 8.528(3)$, $b = 16.433(5)$, $c = 25.757(9)$, $\beta = 97.65(3)°$). Cell parameters (120(1) K) were obtained from 58 reflections with $14° < 2\theta < 24°$. Space groups were determined from systematic absences and subsequent least-squares refinement. Standard reflections (monitored every 100 scans) showed no decay. Lorentz, polarization, and absorption (numerical by use of SHELX76 [48]) corrections were applied. The structures were solved by standard heavy atom techniques with SHELXS and refined with SHELX-93 [49]. Non-hydrogen atoms were refined with anisotropic thermal parameters except C2 and C5 of **7**, which showed non-positive definition. Hydrogen atom positions were calculated and added to the structures factor calculations, but were not refined. Scattering factors, and $\Delta f'$ and $\Delta f''$ values, were taken from literature [50].

5. Supplementary material available

Atomic co-ordinates and ORTEP diagrams for **7** and **8** have been deposited with the Cambridge Crystallographic Data Centre as supplementary publication no. CCDC-103196 and 103197. Copies of the data can be obtained free of charge on request to: The Director, CCDC, 12 Union Road, Cambridge CB2 1EZ, UK (Fax: Int. code +(1223) 336-033; e-mail: deposit@chemcrys.cam.ac.uk). Structure factors and thermal parameters have been deposited with the British Library, Document Supply Centre at Boston Spa, Wetherby, West Yorkshire, LS23, 7BQ, UK, as a supplementary publication and are available on request from the Document Supply Centre. Atomic co-ordinates and equivalent isotropic thermal parameters of hydrogens have been submitted to the Editor.

Acknowledgements

The authors would like to thank the NSF for support of this research.

References

[1] (a) F. Diederich, Y. Rubin, Angew. Chem. 104 (1992) 1123; Angew. Chem. Int. Ed. Engl. 31 (1992) 1101. (b) F. Diederich, Nature (London) 369 (1994) 199.

[2] (a) R.F. Curl, Angew. Chem. 109 (1997) 1636; Angew. Chem. Int. Ed. Engl. 36 (1997) 1567. (b) H. Kroto, Angew. Chem. 109 (1997) 1648; Angew. Chem. Int. Ed. Engl. 36 (1997) 1579. (c) R.E. Smalley, Angew. Chem. 109 (1997) 1666; Angew. Chem. Int. Ed. Engl. 36 (1997) 1595.

[3] Reviews and critical analyses: (a) V.M. Mel'nichenko, A.M. Sladkov, Yu.N. Nikulin, Russ. Chem. Rev. 51 (1982) 421. (b) P.P.K. Smith, P.R. Buseck, Science 216 (1982) 984. (c) See also K. Akagi, M. Nishiguchi, H. Shirakawa, Y. Furukawa, I. Harada, Synthetic Metals 17 (1987) 557.

[4] (a) J.M. Hunter, J.L. Fye, E.J. Roskamp, M.F. Jarrold, J. Phys. Chem. 98 (1994) 1810. (b) R.J. Lagow, J.J. Kampa, H.-C. Wei, S.L. Battle, J.W. Genge, D.A. Laude, C.J. Harper, R. Bau, R.C. Stevens, J.F. Haw, E. Munson, Science 267 (1995) 362. (c) K.-H. Homman, Angew. Chem. 110 (1998) 2572; Angew. Chem. Int. Ed. Engl. 37 (1998) 2435.

[5] Lead references to bending frequencies: (a) C. Liang, L.C. Allen, J. Am. Chem. Soc. 113 (1991) 1873. (b) K. Raghavachari, J.S. Binkley, J. Chem. Phys. 87 (1987) 2191. (c) N.P.G. Roeges, A Guide to the Complete Interpretation of Infrared Spectra of Organic Structures, Wiley, Chichester, 1994, p 226.

[6] B. Bartik, R. Dembinski, T. Bartik, A.M. Arif, J.A. Gladysz, New Journal of Chemistry 21 (1997) 739.

[7] I. Nitta, Acta Crystallogr. 13 (1960) 1035.

[8] B.F. Coles, P.B. Hitchcock, D.R.M. Walton, J. Chem. Soc. Dalton (1975) 442.

[9] M. Altmann, V. Enkelmann, U.H.F. Bunz, Chem. Ber. 129 (1996) 269.

[10] J.T. Lin, J.J. Wu, C.-S. Li, Y.S. Wen, K.-J. Lin, Organometallics 15 (1996) 5028.

[11] Y. Rubin, S.S. Lin, C.B. Knobler, J. Anthony, A.M. Boldi, F. Diederich, J. Am. Chem. Soc. 113 (1991) 6943.

[12] References to C_8–C_{20} complexes prepared in our laboratory: (a) M. Brady, W. Weng, J.A. Gladysz, J. Chem. Soc. Chem. Commun. (1994) 2655. (b) T. Bartik, B. Bartik, M. Jaeger, R. Dembinski, J.A. Gladysz, Angew. Chem. 108 (1996) 467; Angew. Chem. Int. Ed. Engl. 35 (1996) 414. (c) R. Dembinski, T. Bartik, B. Bartik, M. Jaeger, J.A. Gladysz, manuscript in preparation.

[13] References to C_8 complexes prepared in other laboratories: (a) P.J. Kim, H. Masai, K. Sonogashira, N. Hagihara, Inorg. Nucl. Chem. Lett. 6 (1970) 181. (b) F. Coat, C. Lapinte, Organometallics 15 (1996) 477. (c) M.I. Bruce, M. Ke, P.J. Low, B.W. Skelton, A.H. White, Organometallics 17 (1998) 3539. (d) M. Akita, M.-C. Chung, A. Sakurai, S. Sugimoto, M. Terada, M. Tanaka, Y. Moro-oka, Organometallics 16 (1997) 4882.

[14] K. Sonogashira, in: F. Diederich, P.J. Stang (Eds.), Metal Catalysed Cross-coupling Reactions, Wiley-VCH, Weinheim, 1998, p. 204.

[15] (a) R.R. Kostikov, A.Ya. Krasikov, T.V. Mandel'shtam, É.M. Kharicheva, Zh. Org. Khim. 21 (1985) 329. (b) V. Ratovelomanana, Y. Rollin, C. Gébéhenne, C. Gosmini, J. Périchon, Tetrahedron Lett. 35 (1994) 4777.

[16] Precedent for this methodology: H. Hofmeister, K. Annen, H. Laurent, R. Wiechert, Angew. Chem. 96 (1984) 720; Angew. Chem. Int. Ed. Engl. 23 (1984) 727.

[17] W. Weng, T. Bartik, M. Brady, B. Bartik, J.A. Ramsden, A.M. Arif, J.A. Gladysz, J. Am. Chem. Soc. 117 (1995) 11922.

[18] When the solvent is switched to methanol/THF (1:1 v/v), reaction times are reduced by approximately half. This is likely due to enhanced solubility.

[19] Aliquots of solutions of **4** and **6** were analyzed by IR (cm^{-1}, THF): **4**, $\nu_{C\equiv C}$ 2025 m br (range over many experiments, 2010–2028), ν_{NO} 1650 vs.; **6**, $\nu_{C\equiv C}$ 2079 vs., 2043 m, 1895 m, ν_{NO} 1655 vs.

[20] C. Amatore, E. Blart, J.P. Genêt, A. Jutand, S. Lemaire-Audoire, M. Savignac, J. Org. Chem. 60 (1995) 6829. Comparable yields could be obtained with $BrC{\equiv}CSiMe_3$.

[21] (a) B.N. Ghose, Synth. React. Inorg. Met.-Org. Chem. 24 (1994) 29. (b) B.N. Ghose, D.R.M. Walton, Synthesis 12 (1974) 890. (c) R. Eastmond, D.R.M. Walton, Tetrahedron 28 (1972) 4591.
[22] M. Alami, F. Ferri, Tetrahedron Lett. 37 (1996) 2763.
[23] M.D. Bachi, N. Bar-Ner, C.M. Crittell, P.J. Stang, B.J. Williamson, J. Org. Chem. 56 (1991) 3912.
[24] S.-K. Kang, H.-W. Lee, S.-B. Jang, P.-S. Ho, J. Chem. Soc. Chem. Commun. (1996) 835.
[25] T. Tsuda, T. Hashimoto, T. Saegusa, J. Am. Chem. Soc. 94 (1972) 658.
[26] While this study was in progress, another method (involving harsher conditions) for the conversion of alkynyl trimethylsilanes to alkynyl copper species was reported: H. Ito, K. Arimoto, H. Sensui, A. Hosomi, Tetrahedron Lett. 38 (1997) 3977.
[27] J. Manna, K.D. John, M.D. Hopkins, Adv. Organomet. Chem. 38 (1995) 79.
[28] Representative references from an extensive literature: (a) C. Kelley, N. Lugan, M.R. Terry, G.L. Geoffroy, B.S. Haggerty, A.L. Rheingold, J. Am. Chem. Soc. 114 (1992) 6735. (b) J. Ipaktschi, F. Mirzaei, G.J. Demuth-Eberle, J. Beck, M. Serafin, Organometallics 16 (1997) 3965.
[29] D.R. Senn, A. Wong, A.T. Patton, M. Marsi, C.E. Strouse, J.A. Gladysz, J. Am. Chem. Soc. 110 (1988) 6096.
[30] The title compounds in the following papers feature related $^{+}$Re=C=C=C=C=Re^{+} and $^{+}$Re=C=C=C=Mn systems: (a) M. Brady, W. Weng, Y. Zhou, J.W. Seyler, A.J. Amoroso, A.M. Arif, M. Böhme, G. Frenking, J.A. Gladysz, J. Am. Chem. Soc. 119 (1997) 775. (b) T. Bartik, W. Weng, J.A. Ramsden, S. Szafert, S.B. Falloon, A.M. Arif, J.A. Gladysz, J. Am. Chem. Soc. 120 (1998) 11071.
[31] J.A. Ramsden, W. Weng, J.A. Gladysz, Organometallics 11 (1992) 3635.
[32] W. Weng, T. Bartik, M.T. Johnson, A.M. Arif, J.A. Gladysz, Organometallics 14 (1995) 889.
[33] Curiously, the chemical shift trend is reversed at −80°C, as specified for the NMR monitored reaction. Variable temperature ^{1}H-NMR spectra with isolated, purified samples show the same phenomenon (shifts equal at ca. −45°C).
[34] M.F. Summers, L.G. Marzilli, A. Bax, J. Am. Chem. Soc. 108 (1986) 4285.
[35] (a) R. Dunkel, C.L. Mayne, M.P. Foster, C.M. Ireland, D. Li, N.L. Owen, R.J. Pugmire, D.M. Grant, Anal. Chem. 64 (1992) 3150. (b) R. Dunkel, C.L. Mayne, R.J. Pugmire, D.M. Grant, Anal. Chem. 64 (1992) 3133.
[36] (a) K. Kamieńska-Trela, Org. Magn. Res. 14 (1980) 398 (see Table 2). (b) K. Kamieńska-Trela, in: G.A. Webb (Ed.), Annual Reports on NMR Spectroscopy, Academic Press, London, 30 (1995), p. 131. (c) K. Kamieńska-Trela, L. Kania, W. Schilf, L. Balova, Spectrochim. Acta 55A (1999) 817.
[37] H. Jiao, work in progress, Universität Erlangen-Nürnberg.
[38] (a) G.A. Jeffrey, J.S. Rollett, Proc. R. Soc. London Ser. A 213 (1952) 86. (b) T. Lu, M.A. Menelaou, D. Vargas, F.R. Fronczek, N.H. Fischer, Phytochemistry 32 (1993) 1483. (c) U.H.F. Bunz, V. Enkelmann, Organometallics 13 (1994) 3823. (d) V. Enkelmann, Chem. Mat. 6 (1994) 1337. (e) G.P. Jones, P.J. Pauling, J. Chem. Soc. Perkin Trans. II (1979) 1482. (f) E.M. Graham, V.M. Miskowski, J.W. Perry, D.R. Coulter, A.E. Stiegman, W.P. Schaefer, R.E. Marsh, J. Am. Chem. Soc. 111 (1989) 8771. (g) See also K. Inoue, H. Iwamura, Adv. Mater. 4 (1992) 801.
[39] S. Szafert, S.B. Falloon, P. Haquette, work in progress, University of Utah.
[40] W.G. Kofron, L.M. Baclawski, J. Org. Chem. 41 (1976) 1879.
[41] C.R. Jablonski, Aldrichimica Acta 23 (1990) 58.
[42] T_i, initial peak temperature; T_e, extrapolated peak-onset temperature; T_p, maximum peak temperature; H.K. Cammenga, M. Epple, Angew. Chem. 107 (1995) 1284; Angew. Chem. Int. Ed. Engl. 34 (1995) 1171.
[43] A ^{13}C-NMR spectrum of BrC≡C-*p*-C_6H_4Me was also recorded without proton decoupling. From intensity relationships and the magnitude of the coupling to the methyl protons, the 129.2 and 132.0 ppm signals were assigned as *ortho* and *meta* to the methyl group. Similarly, the 139.0 and 119.7 ppm signals were assigned as *ipso* and para to the methyl group. These chemical shift trends were used to assign resonances for the other *p*-tolyl containing compounds.
[44] TLC data (silica gel, hexane:THF 1:1 v/v): (a) Analtech type GF, catalog number 2521, (b) Merck type 60, catalog number 5715.
[45] This represents the downfield line of a partially obscured doublet.
[46] UV–visible spectra were recorded in CH_2Cl_2, and absorbances are in nm (ε, M^{-1} cm^{-1}).
[47] $\underline{m}/\underline{z}$ for most intense peak of isotope envelope; relative intensities are for the specified mass range.
[48] G.M. Sheldrick, SHELX-76, University of Cambridge, UK, 1976.
[49] G.M. Sheldrick, SHELX-93, University of Göttingen, 1993.
[50] D.T. Cromer, J.T. Waber, in: J.A. Ibers, W.C. Hamilton (Eds.), International Tables for X-ray Crystallography; Kynoch, Birmingham, England, 1974; Vol. IV, pp 72–98, 149–150; Tables 2.2B and 2.3.1.